

**Carderock Division
Naval Surface Warfare Center**

Bethesda, Md. 20084-5000

CARDIVNSWC-TR-61-94/17 March 1995

Survivability, Structures, and Materials Directorate
Technical Report

SDTIC
ELECTED
MAY 1 1995
CD

Hot Compression Testing of Tungsten

by
M.G Vassilaros

Hot Compression Testing of Tungsten

CARDIVNSWC-TR-61-94/17

19950427 154



Approved for public release; distribution is unlimited.

CONTENTS

ABSTRACT.....	1
ADMINISTRATIVE INFORMATION.....	1
INTRODUCTION.....	1
MATERIAL.....	2
EXPERIMENTAL PROCEDURE.....	8
RESULTS AND DISCUSSION.....	8
COMPRESSION TEST RESULTS.....	13
ANISOTROPY.....	15
METALLOGRAPHY.....	16
CRACKING.....	16
SUMMARY.....	18
REFERENCES.....	18
DISTRIBUTION LIST.....	65

FIGURES

1. Stress-strain curve for specimen W600-1 tested at 600°F.....	19
2. Stress-strain curve for specimen W800-3 tested at 800°F.....	20
3. Stress-strain curve for specimen W800-3 tested at 800°F.....	21
4. Stress-strain curve for specimen W900-8 tested at 900°F.....	22
5. Stress-strain curve for specimen W900-8 tested at 900°F.....	23
6. Stress-strain curve for specimen W1000-9 tested at 1000°F.....	24
7. Stress-strain curve for specimen W1000-9 tested at 1000°F.....	25
8. Stress-strain curve for specimen W1000-T3 tested at 1000°F...	26
9. Stress-strain curve for specimen W1000-T4 tested at 1000°F...	27
10. Stress-strain curve for specimen W1100-10 tested at 1100°F...	28
11. Stress-strain curve for specimen W1100-10 tested at 1100°F...	29
12. Stress-strain curve for specimen W1230-4 tested at 1230°F....	30
13. Stress-strain curve for specimen W1230-4 tested at 1230°F....	31
14. Stress-strain curve for specimen W1300-11 tested at 1300°F...	32
15. Stress-strain curve for specimen W1300-11 tested at 1300°F...	33
16. Stress-strain curve for specimen W1465-5 tested at 1465°F....	34
17. Stress-strain curve for specimen W1465-5 tested at 1465°F....	35
18. Stress-strain curve for specimen W1700-6 tested at 1700°F....	36
19. Stress-strain curve for specimen W1700-6 tested at 1700°F....	37
20. Stress-strain curve for specimen W1930-7 tested at 1930°F....	38
21. Stress-strain curve for specimen W1930-7 tested at 1930°F....	39
22. Stress-strain curve for specimen W1930-14 tested at 1930°F...	40
23. Stress-strain curve for specimen W1930-14 tested at 1930°F...	41
24. Stress-strain curve for specimen W2158-T1 tested at 2158°F...	42
25. Stress-strain curve for specimen W2158-T1 tested at 2158°F...	43
26. Stress-strain curve for specimen W2158-T2 tested at 2158°F...	44
27. Stress-strain curve for specimen W2158-T2 tested at 2158°F...	45
28. Stress-strain curve for specimen W2400-2 tested at 2400°F....	46
29. Stress-strain curve for specimen W2400-2 tested at 2400°F....	47
30. Stress-strain curve for specimen W3000-12 tested at 3000°F...	48
31. Stress-strain curve for specimen W3000-12 tested at 3000°F...	49
32. 0.2% offset yield strength for tungsten tested at 600 to 3000°F.....	50
33. 5.0% offset yield strength for tungsten tested at 600 to 3000°F.....	51

FIGURES

34. Plastic anisotropy "R" value for tungsten tested at 600 to 3000°F.....	52
35. Photomicrographs of tungsten in "as received" condition.....	53
36. Photomicrographs of tungsten specimen tested at 600°F.....	54
37. Photomicrographs of tungsten specimen tested at 1700°F.....	55
38. Photomicrographs of tungsten specimen tested at 2400°F.....	56
39. Photomicrographs of tungsten specimen tested at 3000°F.....	57
40. Photomicrographs of tungsten specimen tested at 3000°F (longitudinal section) W3000-12.....	58
41. Photomicrographs of tungsten specimen tested at 1100°F (longitudinal section) W1100-10.....	59
42. Photomicrographs of crack in tungsten specimen W600-1 tested at 600°F.....	60
43. Photomicrographs of crack in tungsten specimen W800-3 tested at 800°F.....	61
44. Photomicrographs of crack in tungsten specimen W900-8 tested at 900°F.....	62
45. Photomicrographs of crack in tungsten specimen W1000-9 tested at 1000°F.....	63

TABLES

1. Chemistry of GTE K100 tungsten.....	2
2. Specimen test matrix.....	7
3. Strengths of tungsten in compression at 600 to 3000°F.....	11
4. Plastic anisotropy of tungsten.....	14

Accession For		
NTIS	CRA&I	<input checked="" type="checkbox"/>
DTIC	TAB	<input type="checkbox"/>
Unannounced <input type="checkbox"/>		
Justification _____		
By _____		
Distribution / _____		
Availability Codes		
Dist	Avail and/or Special	
A.I.		

ABSTRACT

A study of the high temperature deformation behavior of tungsten was performed. The cylindrical specimen dimensions were 0.4 inch diameter and 0.6 inch long (10.2 x 15.2 mm) as machined from a tungsten forging. The compression tests were performed in a thermal-mechanical simulator "Gleebel 1500" at temperatures of 600 to 3000°F (315 to 1650°C). The specimens were deformed to a strain of approximately 0.3 with lubricated test fixtures that suppressed any specimen barreling. Compressive stress - stain curves were produced for all specimens and analyzed for 0.2% offset strength as well as 1.0, 2.0 and 5.0% offset strengths. The strengths were observed to decrease with higher temperatures, but appeared to be on a plateau at 50 ksi (345 MPa) in the temperature range of 1200 to 2200°F (650 to 1200°C). The compression specimens tested at or below 1000°F (538°C) experienced cracking. The fracture mode appeared to be intergranular in a single phase microstructure with an elongated grain shape.

ADMINISTRATIVE INFORMATION

This report was prepared under Task Area RS34W53, Task 03, Block SD2A. The work was performed under Work Unit 1-2815-565. The sponsors were Mr. J. G. Toeneboehn (NSWC DD, White Oak), and Mr. R. Garrett, (NSWC Indian Head, White Oak). The report constitutes the completion of the research effort.

INTRODUCTION

The Welding Branch (Code 615) of the Naval Surface Warfare Center (NSWC), Carderock Division, Annapolis Detachment was requested to support Code R31, Dahlgren Division NSWC, White Oak in their investigation of tungsten metal. The use of tungsten as a liner for a shaped charge device has been shown to be advantageous by Brown and co-workers (1993). The use of tungsten, GTE K100, requires the hot forging of sintered powder-metallurgy billets into

the near-net shapes. This forging operation is facilitated with knowledge of the high temperature flow properties of the tungsten. In addition the final application requires a detailed understanding of the work hardening and thermal softening behavior of the material. The purpose of this task was to develop high temperature flow properties from a section of a tungsten forging.

MATERIAL

The forged tungsten was supplied by NSWC White Oak in the form of machined compression specimens. All the specimens were machined from one piece of forged tungsten that had been cut from a shaped charge liner blank. The chemistry of the GTE K100, lot WA263, billet number 124-90 tungsten was supplied by NSWC White Oak and is given in table 1.

Table 1. Chemistry of GTE K100 tungsten

Element	Measured	Maximum allowed in PPM (GTE Spec.)
Al	1	5
Ca	<1	2
Cr	2	10
Cu	<1	2
Fe	9	20
Mg	<1	1
Mn	<1	1
Ni	4	20
Si	2	5
Sn	<1	1
Carbon	10	50
Oxygen	18	50
Nitrogen	10	20

The test program consisted of a series of 17 compression tests performed at a series of temperatures up to 3000°F (1648°C) with cross-head deformation rates of 1.0 and 0.01 inch/second (25.4 and 0.254 mm/second). The supplied tungsten compression samples had the dimensions of 0.40 inches (10.16 mm) in diameter and 0.60 inch (15.24 mm) in height. With these dimensions the initial strain rates of the specimens, assuming constant cross head rate during deformation, would be 1.67 and 0.167 inch/inch. The specimens were removed from the conical shaped liner with the extension of longitudinal axis of the all specimens intersecting the apex of the cone.

The samples were tested in a Gleeble Model 1500 thermal simulator that applies a controlled current through a sample to induce resistance heating. A thermocouple spot welded to the sample surface is used to monitor the temperature and provide input to the temperature control circuit. The control circuit constantly adjusts the magnitude of the current applied to the sample via conductive grips to maintain the specified temperature and heating rate. The Gleeble 1500 was equipped with a high rate servo-hydraulic actuator. The unit was also equipped with a controlled atmosphere chamber that was flooded with argon gas prior to all tests. The test grips within the chamber were flat circular grips of tungsten carbide. These water cooled grips were used to apply load and electrical current for heating. During normal compression or "upset" tests the friction between the specimen ends and grip surfaces prevents the compression specimen cylinders from deforming uniformly in an axisymmetric fashion. The resultant non-uniform deformation is externally manifested as barreling of the cylindrical specimens. To prevent barreling the friction between the specimen and grips must be minimized. This can be accomplished with the use of graphite as a lubricant that can be used at high temperatures in argon and is electrically conductive to accommodate the current applied for resistance heating. Two layers of graphite sheet were used between each end of the specimen and the grips. Between the two graphite sheets was a sheet of tantalum metal that

has a high melting temperature and, for a metal, is a relatively poor thermal conductor. The tantalum and graphite sandwich was utilized to help thermally insulate the compression specimen from the water cooled grips that drew heat from the specimen ends. Without the insulation it is possible to produce a temperature gradient of as much as several hundred degrees along the axial length of the specimen. This temperature distribution would also contribute to the specimen barreling resulting from the higher material strengths of the cooler specimen ends. With the insulation the measured temperature difference between the specimen center and ends was less than 50°F (28°C) after being held at temperature for 60 seconds. This test setup provided the required lubrication and thermal insulation to suppress barreling in all but one compression test (to be discussed later).

Prior to the start of each compression test, the servo-hydraulic piston was disconnected from the machine cross-head and separated by a gap 0.10 inch (2.54 mm). The cross-head held the compression specimen in position with the help of a small air powered positioning ram. The 0.10 inch gap was needed to assure a constant cross-head rate by eliminating the time and travel needed to overcome the piston's inertia prior to the beginning of the specimen loading. During the compression tests the time, load, cross head position, and specimen diameter were continuously monitored and digitally recorded with a high rate data acquisition system. The acquisition system was integral to the Gleeble 1500 and had 12 bit resolution on each channel. The test data was downloaded from the acquisition system's memory to a disk on a desk-top computer after each test. The data was then translated into ASCII format and imported to a spreadsheet program for analysis. The data analysis included calculating the true stress, true diametral strain, and true longitudinal strain. The measured specimen temperature and compression rate were checked. The true stress was calculated using equation 1, which uses the measured load divided by the cross sectional area calculated from the initial diameter plus the measured change in diameter from the "C-

strain" diametral gage.

$$\sigma_{\text{true}} = P_i / (\pi * (\text{Dia}_o + C_i)^2 / 4) \quad \text{Eq. 1)$$

σ_{true} = True Stress

P_i = Measured load

Dia_o = Initial specimen diameter

C_i = Measured change in diameter

The measured change in diameter, C_i , was obtained from a "C-strain" gage attached to the center of the compression specimen. The gage measured the diameter change in only one orientation. The tungsten specimens had a plastic anisotropy that produced an oval shape in the final cross section of the specimen. The final diameter (Dia_f) of the specimen was calculated from the average of the measured final minimum and final maximum diameter of the oval shaped specimen cross section. It was assumed that the rate of change from the initial diameter to the final diameter of the specimen at any orientation was the same if linearly normalized with the final diameter of that orientation. Therefore, the change of diameter at any orientation with respect to time would have the same shape if the change in diameter was normalized with the final diameter at that orientation. Additionally, the change in diameter as a function of time at the orientation corresponding to the position of the "C-strain" gage could be used to describe the behavior at any other orientation (called X) by multiplying all the values by $(\text{Dia}_f \text{ at } X) / (\text{Dia}_f \text{ at gage})$. These assumptions were used by the author to adjust the output of the "C-strain" diameter gage to reflect more closely the instantaneous change in the average diameter of the compression specimen.

The true strain (diametral) was calculated using the measured change in diameter and the initial diameter as in equation 2.

$$\epsilon_d = 2 * \ln((\text{Dia}_o + C_i) / \text{Dia}_o) \quad \text{Eq. 2)$$

ϵ_d = True diametral strain

C_i = Measured change in diameter

Dia_o = Initial specimen diameter

The true longitudinal strain of the specimen was calculated from the engineering strain as shown in equation 3.

$$\epsilon_L = \ln(1 + (L_o - l_i) / L_o) \quad \text{Eq. 3)$$

ϵ_L = True longitudinal strain

L_o = Original specimen length

l_i = Change in cross head position

Whenever possible plots of true stress versus true strain were made for both the diametral and longitudinal data. In a few cases the diametral data was incomplete due to large splits (failure) in the specimens that affected both the measurement of the true diametral strain and the true stress leaving only longitudinal engineering strain and engineering stress.

After the specimens were upset tested, they were measured for final length and diameters (minimum and maximum). In some cases the orientation of the diameters with respect to the original surface of the tungsten part was recorded. All the specimens were metallographically examined after deformation for general microstructure. Specimens which displayed any cracking were metallographically examined for crack path and orientation.

Table 2. Specimen test matrix.

Specimen Identification	Test Temperature in °F (°C)	Test Cross Head Rate in./sec. (mm/sec.)
W1000-T1	1000 (538)	1.0 (25.4)
W1000-T2	1000 (538)	1.0 (25.4)
W2158-T3	2158 (1181)	1.0 (25.4)
W2158-T4	2158 (1181)	1.0 (25.4)
W600 - 1	600 (315)	1.0 (25.4)
W2400- 2	2400 (1316)	1.0 (25.4)
W800 - 3	800 (427)	1.0 (25.4)
W1230- 4	2130 (1166)	1.0 (25.4)
W1465- 5	1465 (796)	1.0 (25.4)
W1700- 6	1700 (927)	1.0 (25.4)
W1930- 7	1930 (1054)	1.0 (25.4)
W900 - 8	900 (482)	1.0 (25.4)
W1000- 9	1000 (538)	1.0 (25.4)
W1100-10	1100 (593)	1.0 (25.4)
W1300-11	1300 (704)	1.0 (25.4)
W3000-12	3000 (1649)	1.0 (25.4)
W1930-14	1930 (1054)	0.01 (0.254)

RESULTS AND DISCUSSION

COMPRESSION TEST RESULTS

The tungsten compression specimens tested were received in two different batches. The first batch of four specimens was tested at temperatures of 1000 and 2158°F (538 and 1181°C), two at each temperature as shown in Table 1 (specimen id. ending T1-T4). The second batch of compression specimens (specimen id. ending in 1-14) were tested over a range of temperatures from 600 to 3000°F (315 to 1649°C) as shown in Table 1. All but specimen W1930-14 were tested with an applied cross head travel rate of 1.0 inch per second that produced a strain rate of 1.67 in/in/second. Sample W1930-14 was tested with a cross head rate of 0.01 in per second that produced a strain rate of 0.0167 in/in/second. A sample designated W1930-13 was to be tested with a cross head rate of 0.1 inch/second but the test was unsuccessful and no test data was produced.

The 17 hot compression tests that were successfully performed produced the stress strain curves shown in figures 1 through 31. Three of the 17 specimens split in half along the plane intersecting the diameter and longitudinal axis of the specimen. The splitting of specimens W600-1, W1000-T3 and W1000-T4 produced two semi-circular specimens during specimen yielding. The semi-circular specimens had a length to width of greater than the original 1.5 that caused the specimens to be unstable and buckle. This behavior produced erroneous diametral gage (C-Strain) results that were recorded but not shown. Without the correct diametral

data the true stress and diametral strain could not be calculated. This splitting behavior of these three specimen resulted in output of only longitudinal data instead of both diametral and longitudinal data as from the other 14 specimens.

The splitting of the tungsten specimens occurred at 600 °F (315°C) and 1000°F (538°C). Small cracks with splits were observed with test temperatures of 800, 900 and 1000°F (427, 482 and 538°C) in specimens W800-3, W900-8 and W1000-9. The two 1000°F specimens (W1000-T3 and W1000-T4) which split were from the first batch of 4 specimens. The other 4 specimens that cracked (W600-1, W800-2, W1000-9 and W1000-10) were cut from a different section of the same tungsten part. Tietz and Wilson (1965) reported on the ductile-to-brittle fracture behavior of powder-metallurgy (PM) tungsten in various conditions and indicated that brittle behavior can be observed at temperatures as high as 500 C (932 F). However some of their PM tungsten was exhibiting fully ductile behavior to temperatures as low as 300 C (572 F) in quasi-static tests.

For all the 17 specimens tested there was produced a stress-strain curve from the cross head displacement data. These curves were marked as (longitudinal). The data was not corrected for system compliance, which includes the elastic deformations of the specimen, grips and fixtures. This results in a low calculated elastic modulus. The stress-strain curves produced from the diametral (C-strain) data were marked (diametral). These curves had much higher elastic and more realistic modulus values since the system compliance was not part of the displacements measured by the

diametral gage. In examining any pair of stress-strain curves from one specimen the curve with the lower elastic modulus will be marked as (longitudinal).

The compression test performed at 3000°F (1649°C) was not a complete success. The specimen experienced some barrelling and broke the tungsten-carbide test fixtures during the test. The specimen data did produce two stress-strain curves but the curves have some error associated with them at most strains beyond yield.

The stress-strain curves shown in figures 1-17 were analyzed to calculate the off-set strengths at values of 0.02%, 1.0%, 2.0% and 5.0% strain. These values are listed in table 3 with any remarks concerning the cracking behavior of the specimens.

Table 3. Strengths of tungsten in compression at 600 to 3000°F

Specimen Identification and strain gage	Test Temp. °F	Strength, @0.2% ksi	Strength, @1.0% ksi	Strength, @2.0% ksi	Strength, @5.0% ksi	Remarks
W600 - 1, long.	600	95.0	--	--	--	Split
W800 - 3, long.	800	92.0	96.0	99.7	104.8	2 Crack
W900 - 8, diam.	900	67.7	82.1	85.9	93.2	1 Crack
long.	900	67.6	78.8	84.2	91.9	
W1000- 9, diam.	1000	53.2	64.0	75.5	81.5	1 Crack
long.	1000	60.0	65.5	73.6	83.8	
W1000-T4 long.	1000	56.0	63.6	72.4	86.5	Split
W1000-T3 long.	1000	59.0	--	--	--	Split
W1100-10, diam.	1100	64.0	71.3	76.2	83.7	
long.	1100	63.7	67.7	72.5	82.4	
W1230- 4, diam.	1230	56.0	65.8	68.6	76.4	
W1300-11, diam.	1300	56.5	61.5	65.6	73.5	
long.	1300	55.4	59.4	61.7	71.5	
W1465- 5, diam.	1465	54.6	62.8	66.8	71.3	
long.	1465	52.2	54.2	57.6	68.3	
W1700- 6, diam.	1700	50.6	54.6	58.6	64.2	
long.	1700	46.0	50.0	50.8	59.5	
W1930- 7, diam.	1930	49.9	53.9	56.5	60.2	
long.	1930	41.0	47.8	51.3	57.4	
W1930-14, diam.	1930	46.0	47.6	48.8	50.7	
long.	1930	44.2	46.3	47.6	50.1	
W2158-T1, diam.	2158	47.3	57.5	60.1	60.9	
W2158-T2, diam.	2158	50.2	56.3	58.7	62.6	
W2400- 2, diam.	2398	39.1	46.0	47.5	50.5	
long.	2398	35.0	40.0	46.5	49.5	
W3000-12, diam.	3000	18.6	19.5	22.0	26.0	broken
long.	3000	11.5	14.9	18.5	20.4	fixture

The 0.2% offset yield strengths listed in table 3 from the longitudinal and diametral stress-strain curves were usually within 12% of each other except specimens W1930-7 and W3000-12. These errors were usually associated with small variation in the early yielding portion of the curves. These errors usually decreased with strain to less than 5% difference. The test that had the largest error between 0.2% offset yields strengths from diametral and longitudinal was W3000-12. The longitudinal curve was significantly lower than the diametral most likely due to the yielding of the tungsten-carbide grips that failed during test. At 3000°F the tungsten carbide must have a lower yield strength than the pure tungsten.

The 0.2% offset yield strengths versus test temperatures were plotted in figure 32. The largest change in yield strength occurs from 600 to 900°F as the strength drops about 20 ksi that gives a change of -0.067 ksi/°F. The temperature range from 1000 to 2158°F displays a region of temperature resistance with a strength drop of about 10 ksi that results in a strength change of -0.0086 ksi/°F. In the temperature range beyond 2158°F to 3000°F there is a drop in strength of 30 ksi which produces a strength change of -0.036 ksi/°F. Results were published by Ryan and Dowding (1993) concerning similar compression tests performed on a 4.55 Ni -1.97 Fe -2.75 Co -tungsten alloy. Their results also showed a large drop in strength from room temperature to 932 F (500C). The room temperature yields strength of the tungsten alloy was 135 to 145 ksi (915 to 1000 MPa). The yield strength dropped to approximately 62 ksi (420 MPa) at 932 F (500 C). Although the tungsten alloy had a much high room temperature strength than the pure tungsten alloy, the high temperature strengths in the range of 925 to 1832 (500 to 1000 C) were in a similar range when tested at the slower strain rates of 10^{-2} to 10^{-1} sec $^{-1}$.

The 5.0% offset strengths versus test temperatures were plotted in figure 33. The shape of the curve similar to the 0.2% data shown in figure 32 that appears to have a shelf in strength around 2000°F. For forging purposes it appears that there is

little difference in choice of forging temperatures in the range of 1500 to 2200°F (815 to 1200°C) since this range has similar flow properties.

STRAIN RATE EFFECT

Two hot compression test were performed at the same temperature but with different strain rates. Specimen W1930-7 was deformed with a cross-head rate of 1.0 inch/sec., while specimen W1930-14 was deformed at 0.01 inch/sec. The stress-strain curves for the specimens are shown in figures 20 through 23 and the tabulated strengths are listed in table 3. Examination of the curves and measured strength indicated that there is an effect of the applied strain rate on strength. The specimen W1930-7 tested at the faster rate was higher in 0.2% to 5% offset yield strengths than the W1930-14 tested at the slower rate. The difference in strength ranged 3-4 ksi at 0.2% yield to 7-9 ksi at 5% yield strength. The initial yield strength was higher and the hardening rate was higher with the faster loading rate.

ANISOTROPY

The final diameter measurements of the compression samples suggest that there was plastic anisotropy in flow behavior. The maximum final diameter divided by the minimum final diameter of the sample called the R-value was plotted as a function of temperature for the samples tested. The results are shown in figure 34 and tabulated in table 4. The data indicate that the R-value increases with temperature and does not display any plateau region as seen with the strength measurements. The anisotropy values were measured with respect to the specimen orientation to the outer surface of the original forging. Some specimens were supplied with a mark on the area of the circumferential surface that was closest to the outer surface of the forging. The position of the mark was maintained through the testing and recorded with respect to the direction of the maximum R value. The orientation mark and direction of maximum R value were also monitored with respect to

the specimen position in the compression test fixture. Both sets of measured angles are listed in table 4. Of the 12 specimens analyzed 9 displayed a maximum R value direction within 25 degrees of the outer wall mark. All the specimen analyzed were within 45 degrees of the original outer wall of the forging. The orientation of the specimen with respect to random placement within the compression test fixtures produced no preferred orientation. These results indicate that the plastic anisotropy observed in these compression test may be the result of a texture or preferred grain orientation in the tungsten part.

Table 4. Plastic anisotropy of tungsten.

Specimen Identification	Test Temperature °F	R-Value Max/min	<u>Angle between specimen reference mark and</u>		Top of Test Fixture degrees
			Maximum Diameter degrees	10	
W800 -3 long	800	1.025			180
W900 -8	900	1.042	45		230
W1000-9	1000	1.038	30		0
W1100-10	1100	1.032	0		240
W1230-4	1230	1.067	45		135
W1300-11	1300	1.066	20		135
W1465-5	1465	1.039	22		225
W1700-6	1700	1.061	10		180
W1930-7	1925	1.059	0		135
W1930-14s	1935	1.089	0		300
W2400-2	2398	1.074	20		270
W3000-12	3000	1.121	10		110

METALLOGRAPHY

After the tests were completed a metallographic analysis was performed on the compression specimens that were in the second batch. These included all specimens that did not have a "T" in the specimen identification. Besides these 13 specimens an untested piece of tungsten was examined as representative of "as received" material. The 14 samples were sectioned, polished and etched with Murakami's etchant to reveal the general microstructure. The microstructure of the as-received tungsten is shown in figure 35. The figure includes a 50X and 500X photomicrograph. The structure of the tungsten appears to be single phase with an elongated grain structure. The grain width appears 5 to 20 μm and the length is 10 to 50 μm . The elongated nature and lack of equiaxed grains would suggest that the material has seen some deformation at a temperature below its recrystallization temperature. Figures 36, 37 and 38 are photomicrographs of tungsten specimens tested at 600, 1700, and 2400°F. Compared to the as received material, there appears to be very little change in either the extent of the elongation or the general grain size. This was true of all the microstructures of specimens tested at or below 2400°F. The effect of a 30% increase in the cross sectional area resulting from the compression tests would cause an increase in grain dimensions for the cross section shown of approximately 15% that would be too small to be noticed by eye in such a microstructure. One main effect of a high temperature environment on microstructure would be recrystallization. This would lead to the appearance of some or all grains to become equiaxed. This effect was not observed in any of the microstructures from specimens tested at 2400°F or less.

The specimen W3000-12 was tested at 3000°F. Figure 39 is the photomicrographs of this specimen's microstructure. The tungsten has been recrystallized. The specimen may have recrystallized immediately after the compression test was performed. This would account for the specimen anisotropy behavior being consistent with the lower temperature specimens as shown in figure 34. However, the W3000-12 was sectioned longitudinally, and examined

metallographically as shown in figure 40. For comparison purposes the same procedure was performed on specimen W1100-10 and the results are shown in figure 41. Examination of the photomicrographs of specimen W3000-12 in figure 40 reveals the microstructure had recrystallized and achieved some amount of grain growth. The figure also shows that the new grains do not appear to be equiaxed as would be expected but to have some grain elongation which would not be expected if the material recrystallized after deformation. The grain elongation is in the direction perpendicular to the longitudinal axis of the specimen. The elongation was not inherited from the deformed structure because the unrecrystallized structure displays a grain elongation in the longitudinal direction as shown in figure 41 which was the result of the deformation of the forging. Additionally any grain elongation apparent in the original structure should disappear with some grain growth which deletes the old grain boundaries. The elongated grains of the recrystallized microstructure appears to indicate that the tungsten recrystallized at 3000F during the 1 minute hold prior to deformation in the Gleeble. Therefore the deformed appearance in the microstructure is the result of the compression test deformation which also indicates that the plastic anisotropy values measure does not depend upon the originally deformed microstructure. The testing of a recrystallized tungsten specimen at 3000F may also account for the measured yield strength which was much lower than predicted by a extension of the data from the specimens tested at lower tmeperature which did not show any evidence of recrystallization.

CRACKING

As shown in table 3, the tungsten specimens tested at or below 1000°F experienced cracking and splitting. Specimens W600-1, W800-3, W900-8 and W1000-9 were examined metallographically to determine the nature of the cracking. Examinations of the photomicrographs (figures 42, 43, 44 and 45) of the four specimens indicate that they all displayed intergranular cracking. Tungsten, like steel

and all other body-center-cubic (BCC) structure metals, can display a ductile-to-brittle fracture mode transition. Properly performed compression specimen tests that do not display any barrelling should not have any major tensile stresses that could cause fracture. However small frictional effects combined with Poisson's stresses have combined to produce enough tensile stress to cause cracking of tungsten at temperatures as high as 1000°F. This would suggest that tungsten has a very low intergranular fracture stress. It is therefore reasonable to assume that brittle fracture of tungsten can occur at temperature greater than 1000°F if a major tensile stress is applied to the metal. It therefore appears that forging a temperature of much higher than 1000°F would be necessary to deform tungsten without any cracking.

SUMMARY

A series of hot compression tests were performed on 17 cylindrical tungsten specimens. The tests were performed at temperatures of 600 to 3000°F (315 to 1650°C) with graphite lubrication. The tests results were in the form of compressive stress-strain curves to total strains of approximately 30%. The 0.2% offset yield strengths of the tungsten ranged from 95 to 18 ksi (655 to 128 MPa) with an apparent "shelf strength" of approximately 50 ksi (345 MPa) at temperatures of 1200 to 2200°F (650 to 1200°C). The specimens did not deform in a radially symmetric fashion but displayed plastic anisotropy that increased with test temperature. Test temperatures of 2400°F (1315°C) or less did not cause any apparent changes in microstructure. A test temperature of 3000°F produced a recrystallized microstructure. The tungsten specimens exhibited some cracking in specimens tested at or below 1000°F (537°C). The cracking often leads to the specimen splitting. The cracking appeared to be intergranular in nature.

REFERENCES

Rayn, K. F. and R. J. Dowding, Tungsten and Tungsten Alloys - 1992, Ed. A. Bose and R.J. Dowding, 1993, p. 249-256

Brown, R. E., M. E. Majenus, and J. S. Lewis, Tungsten and Tungsten Alloys - 1992, Ed. A. Bose and R. J. Dowding, 1993, p. 447-454

Tietz, T. E. and J. W. Wilson, Behavior and Properties of Refractory Metals, Stanford University Press, 1965, p. 287

W600-1

Eng. Stress-True Strain (Longitudinal)

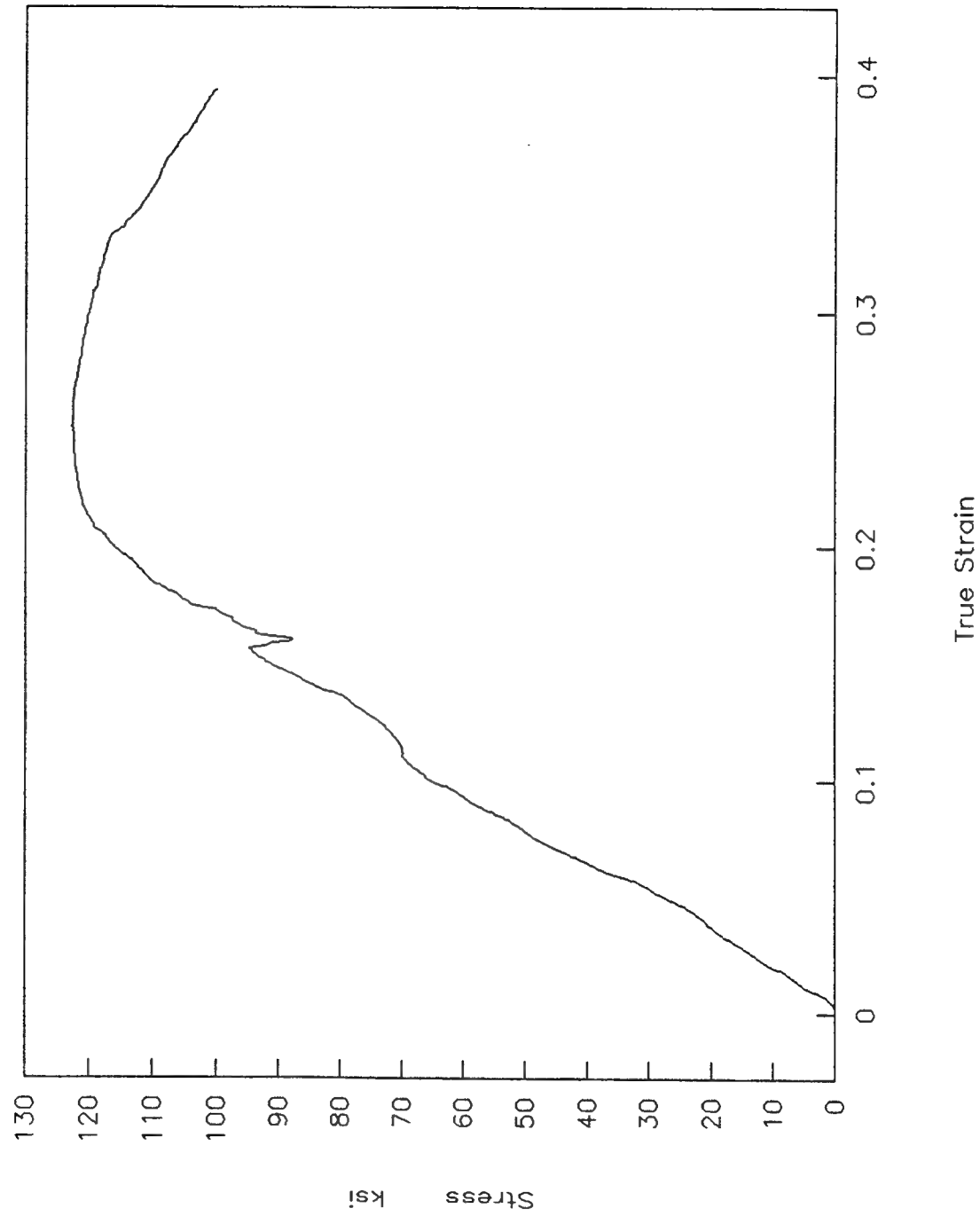


Figure 1. Stress - strain curve for specimen W600-1 tested at 600°F.

W800-3

True Stress - True Strain (diametral)

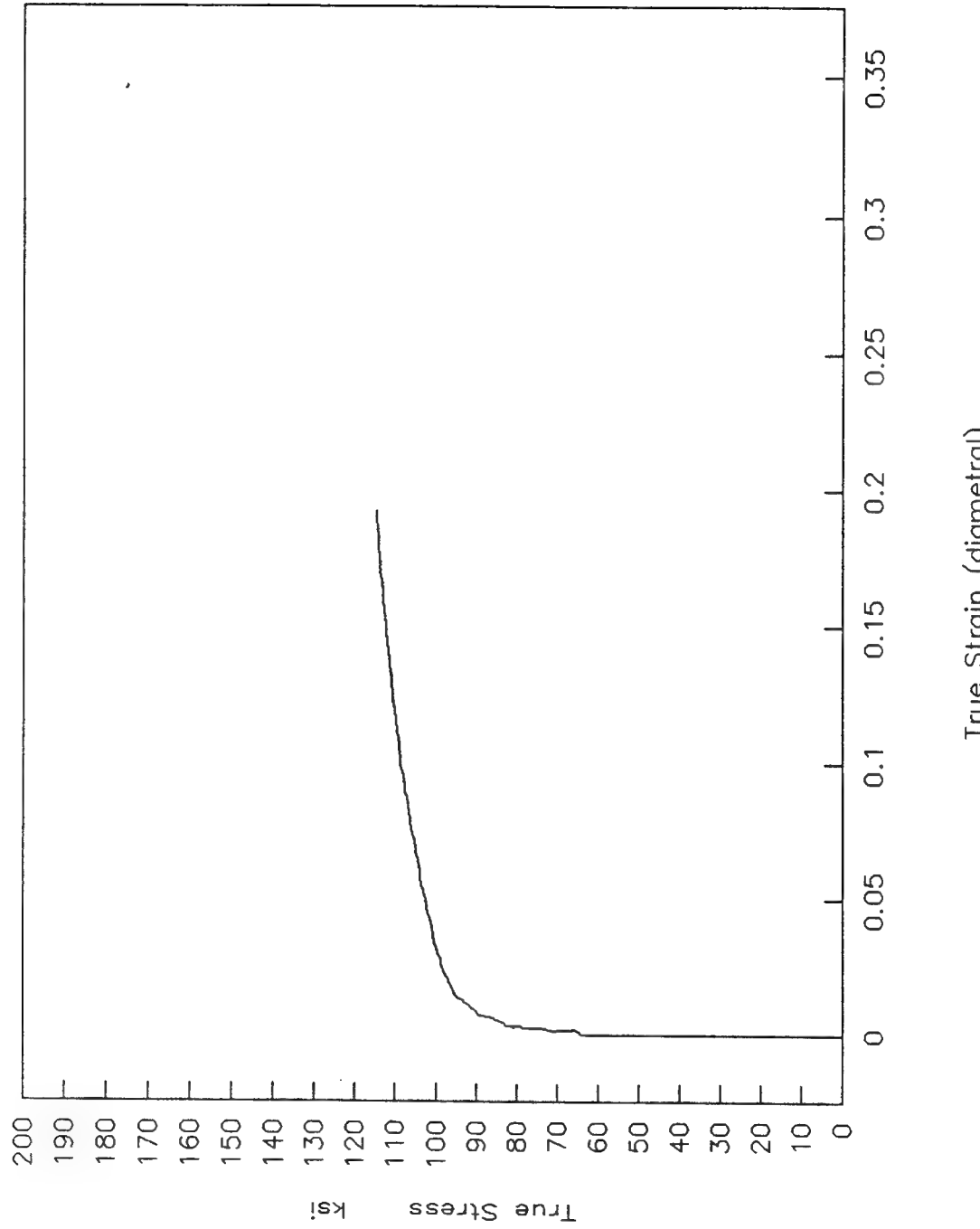


Figure 2. Stress - strain curve for specimen W800-3 tested at 800°F.

W800-3

True Stress-True Strain (longitudinal)

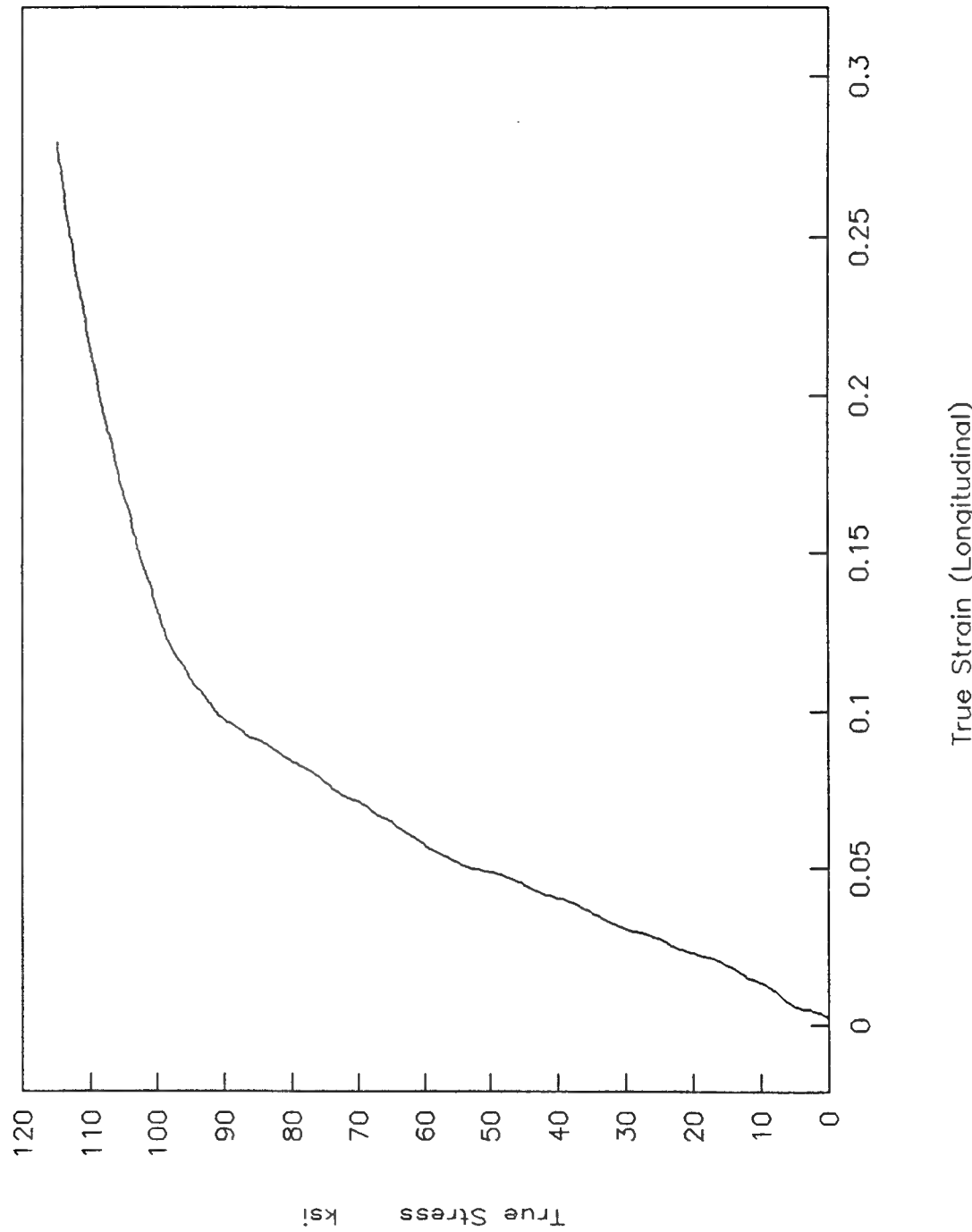


Figure 3. Stress - strain curve for specimen W800-3 tested at 800°F.

W900-8

True Stress - True Strain (diametral)

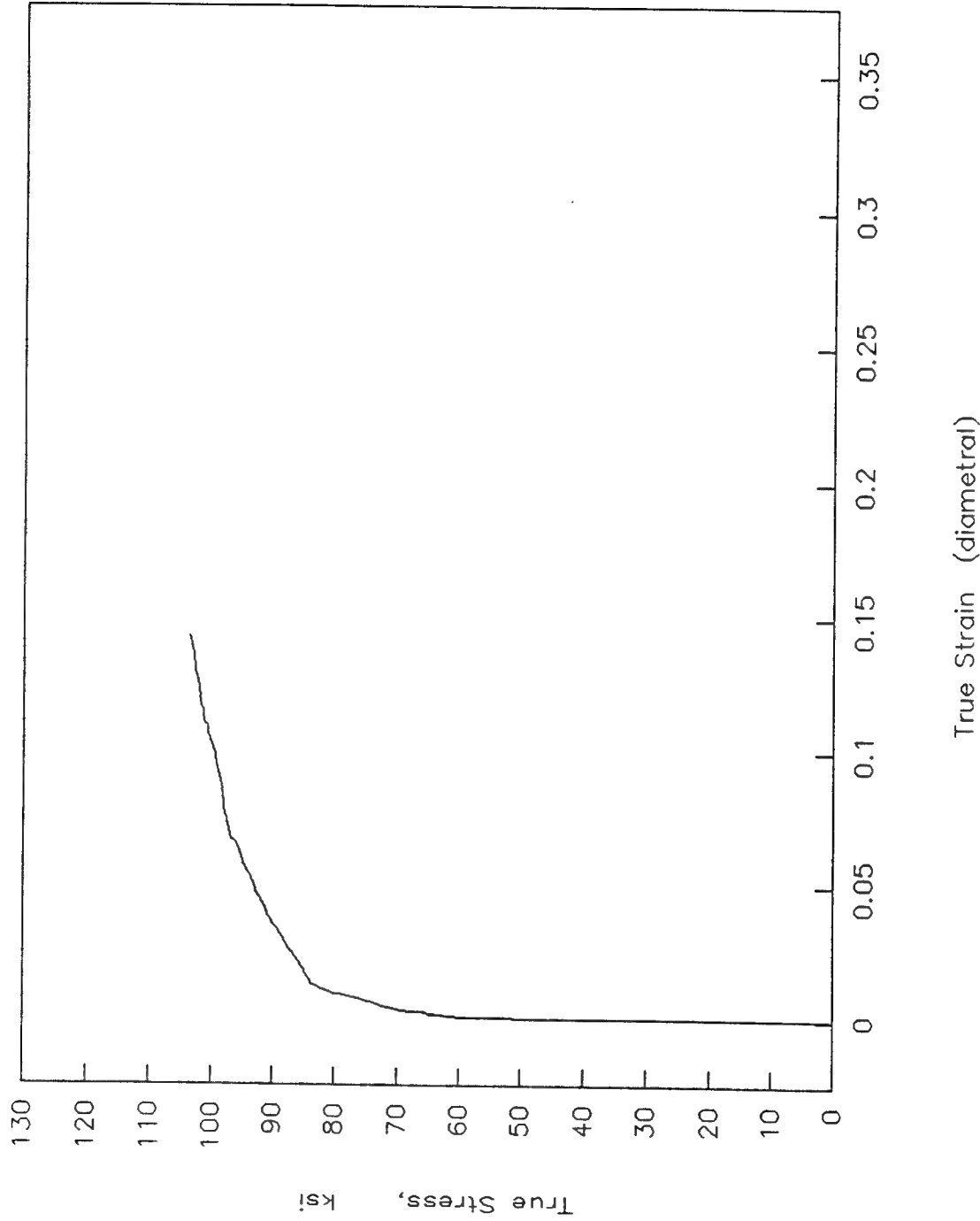


Figure 4. Stress - strain curve for specimen W900-8 tested at 900°F.

W900-8

True Stress-True Strain (longitudinal)

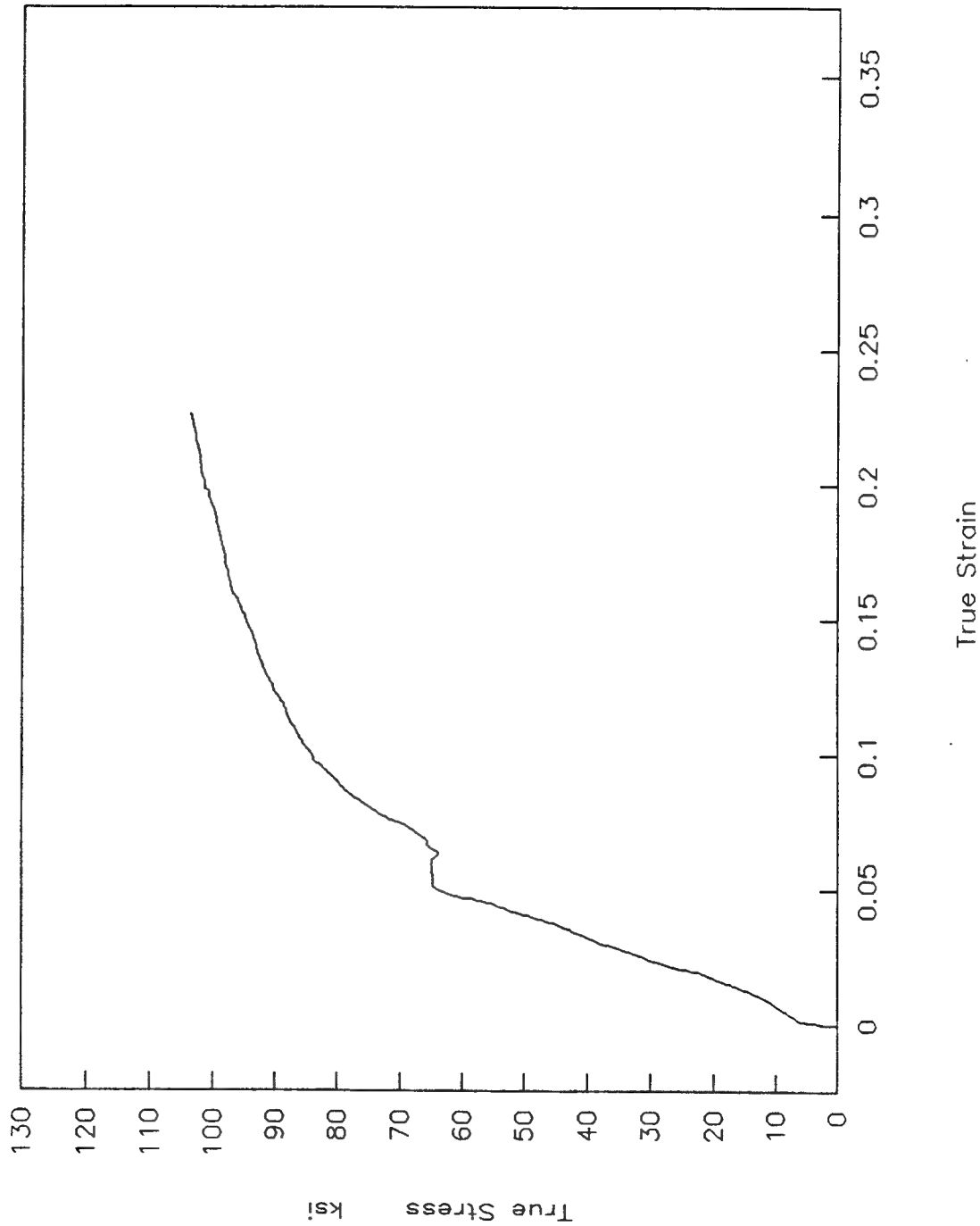


Figure 5. Stress - strain curve for specimen W900-8 tested at 900°F.

W1000-9

True Stress - True Strain (diametral)

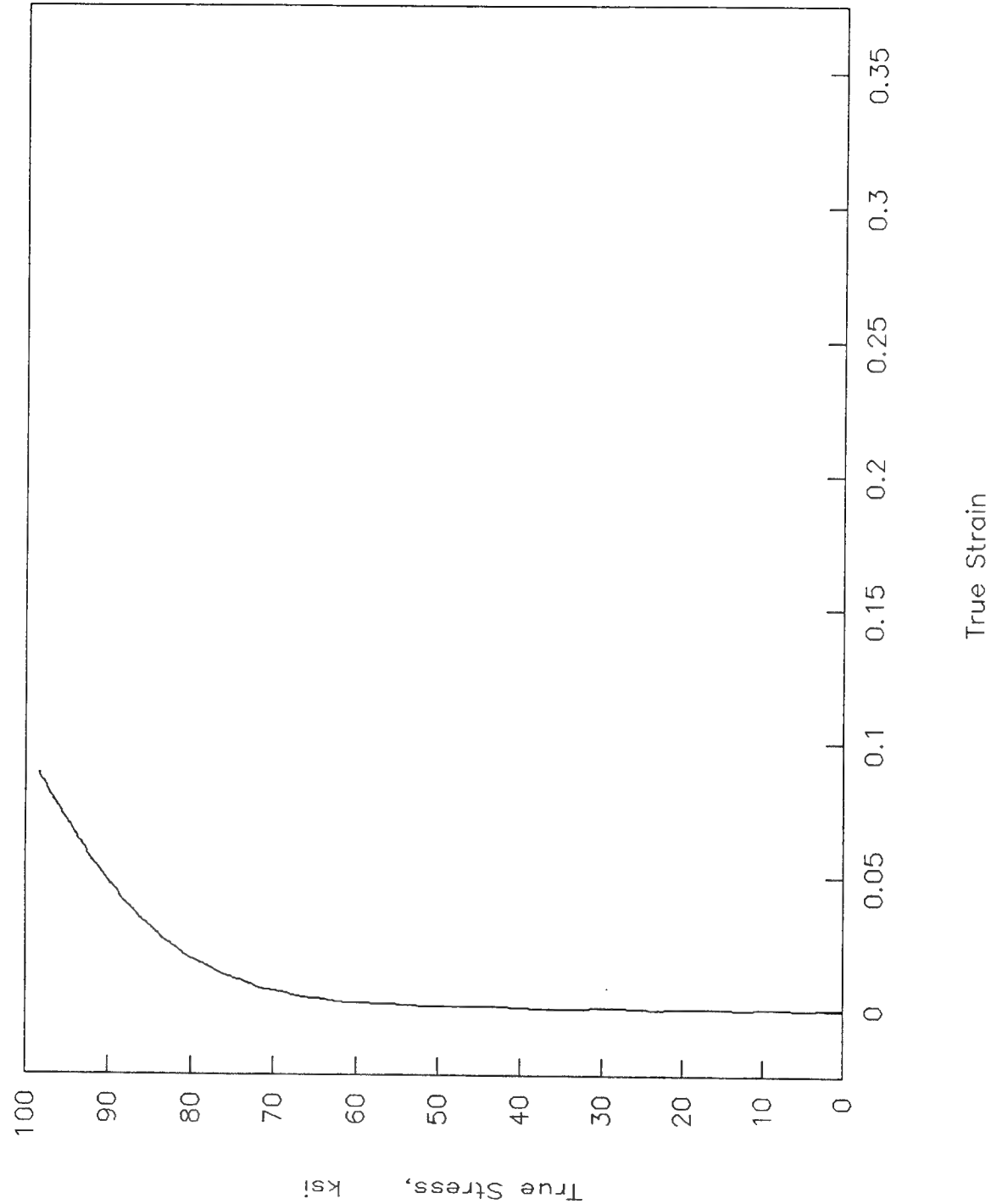


Figure 6. Stress - strain curve for specimen W1000-9 tested at 1000°F.

W1000-9
True Stress-True Strain (longitudinal)

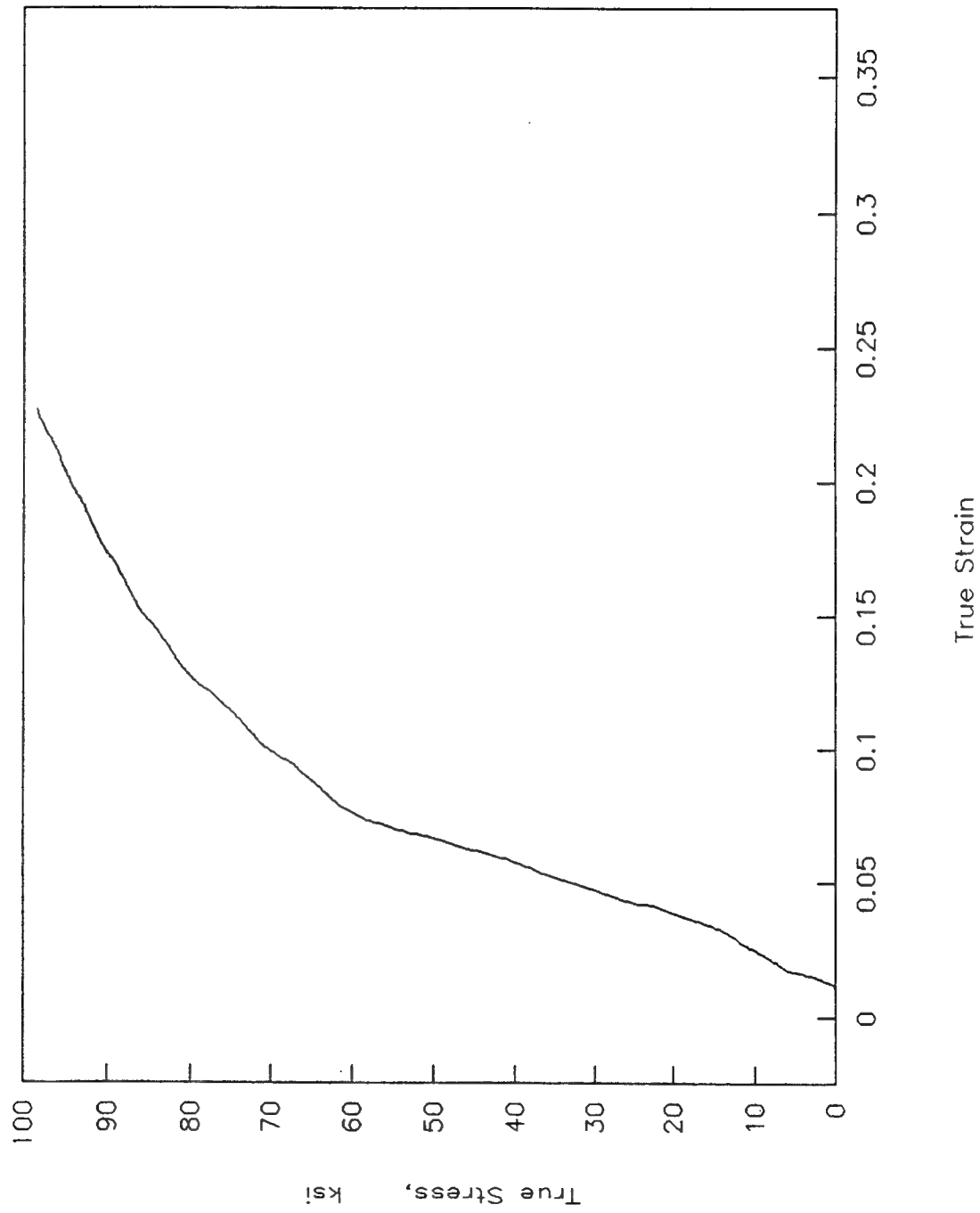


Figure 7. Stress - strain curve for specimen W1000-9 tested at 1000°F.

W1000-T3

True Stress-True Strain (longitudinal)

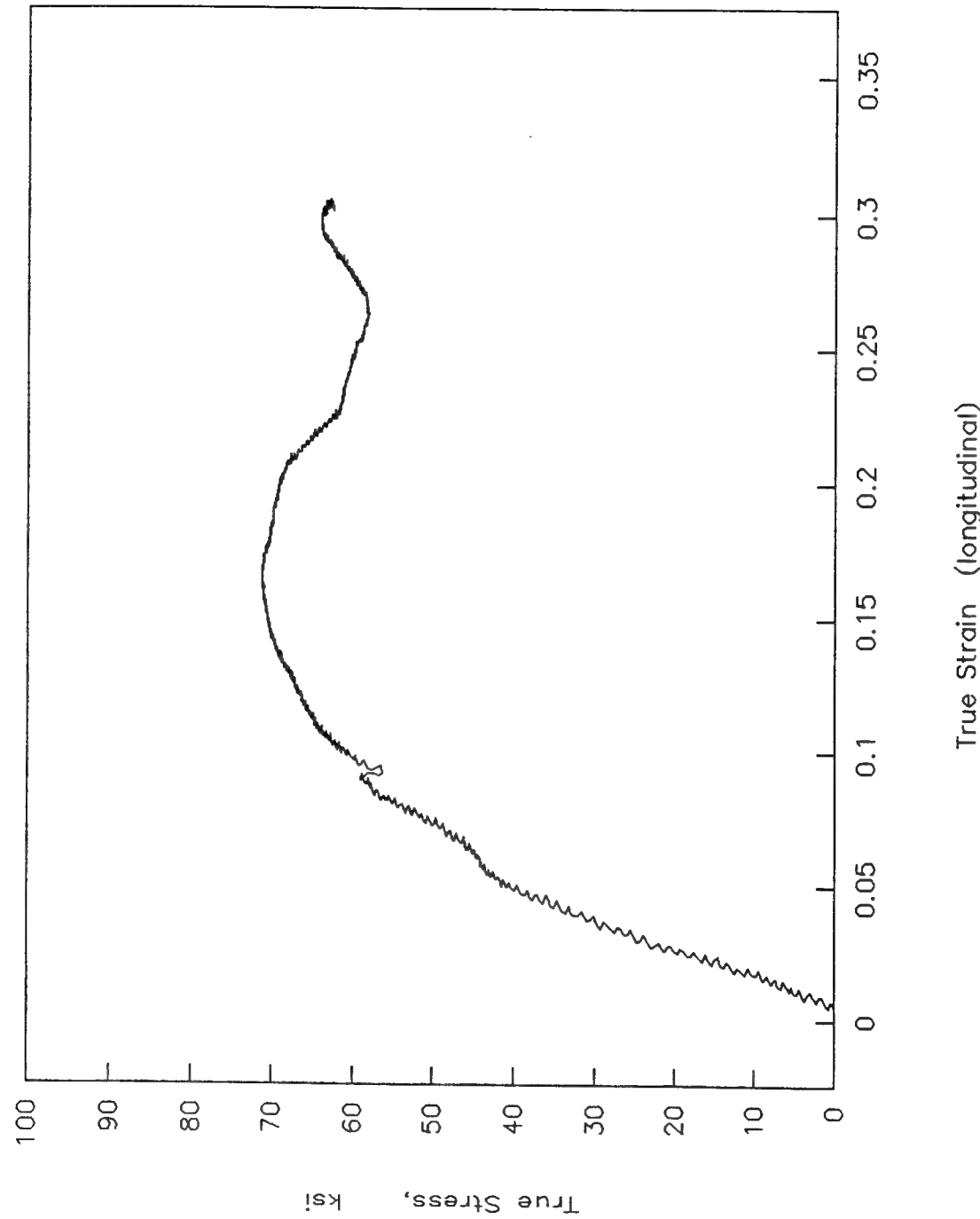


Figure 8. Stress - strain curve for specimen W1000-T3 tested at 1000°F.

W1000-T4
Engineer Stress—True Strain (long.)

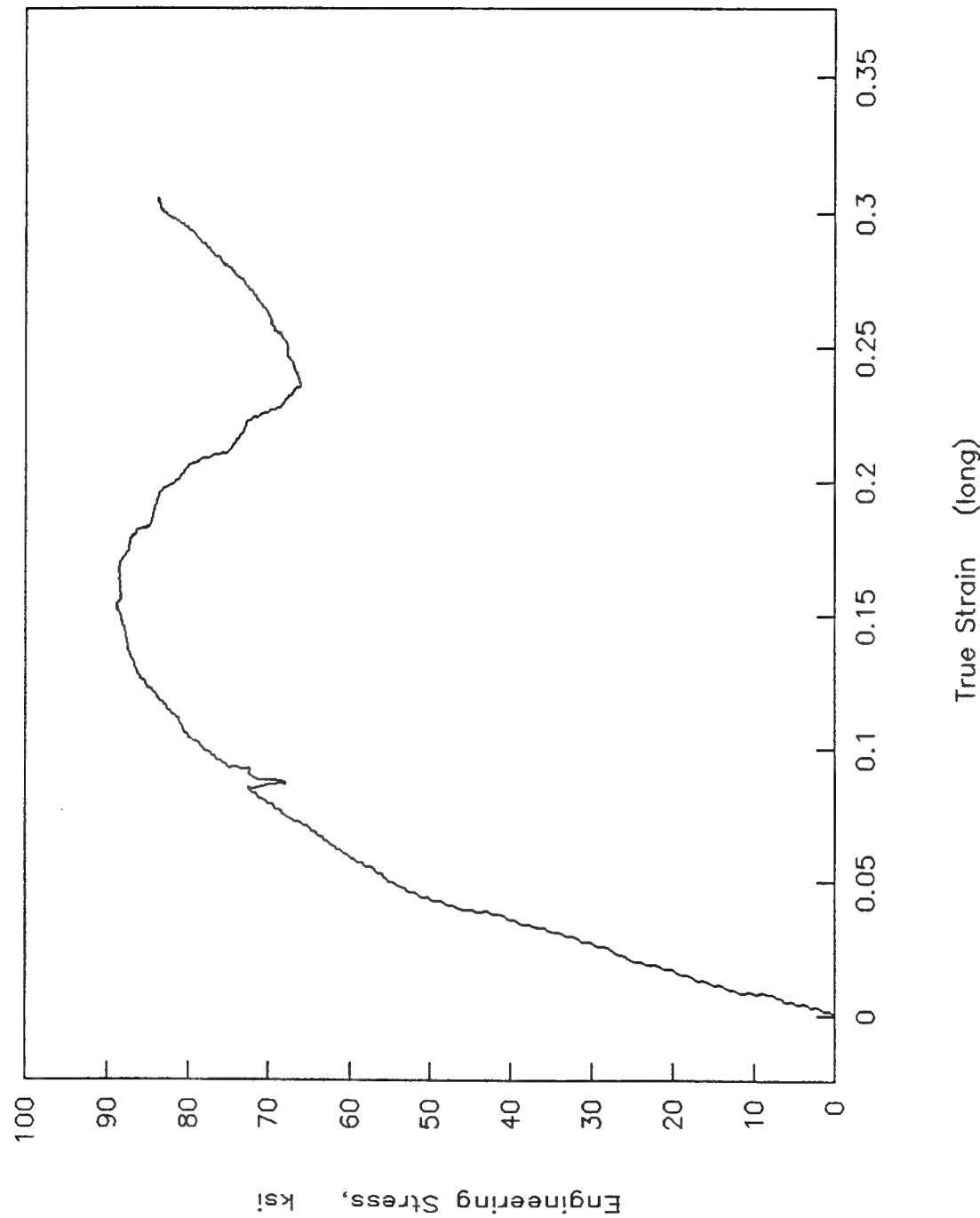


Figure 9. Stress - strain curve for specimen W1000-T4 tested at 1000°F.

W1100-10
True Stress - True Strain (diametral)

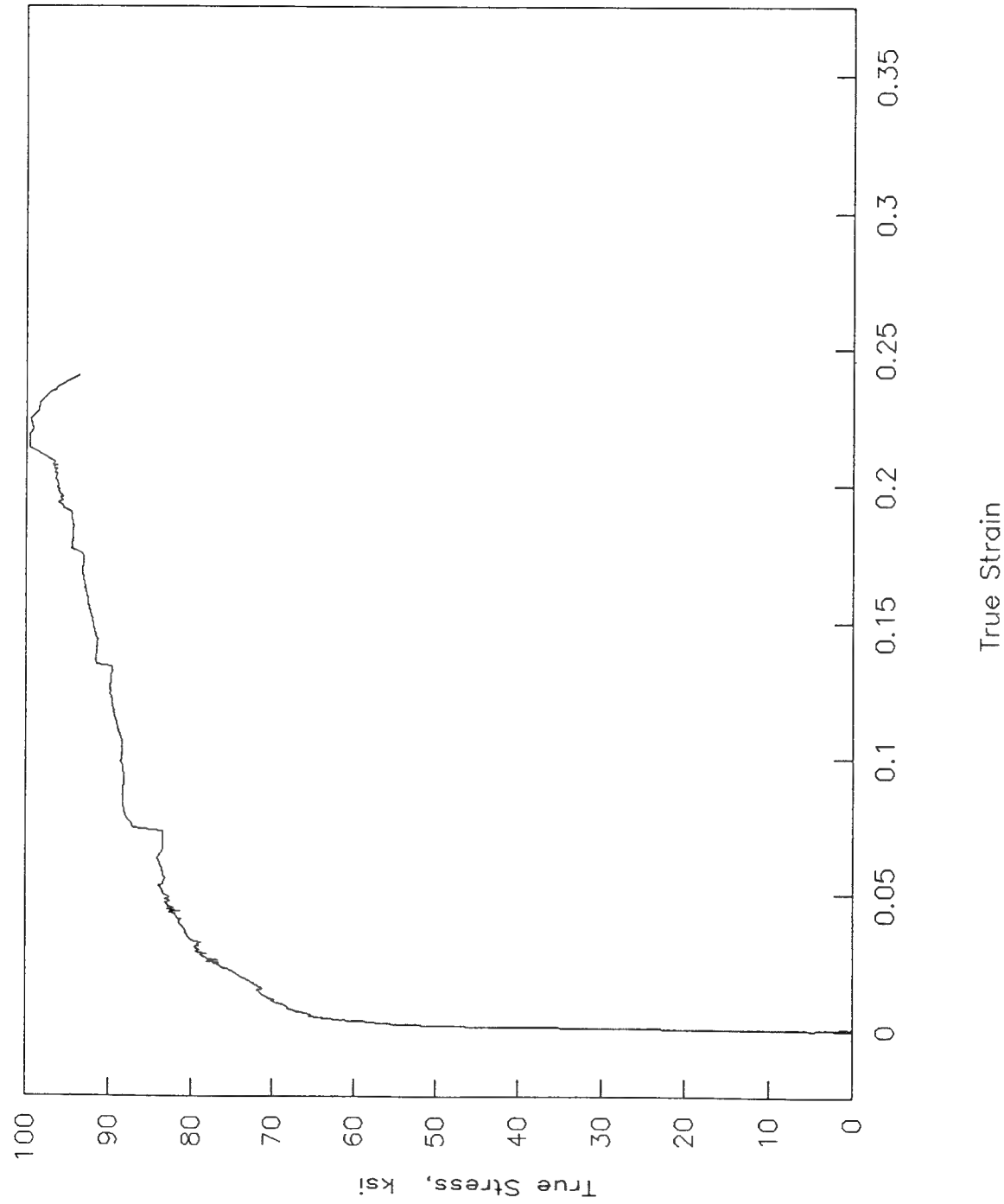


Figure 10. Stress - strain curve for specimen W1100-10 tested at 1100°F.

W 1100-10

True Stress—True Strain (longitudinal)

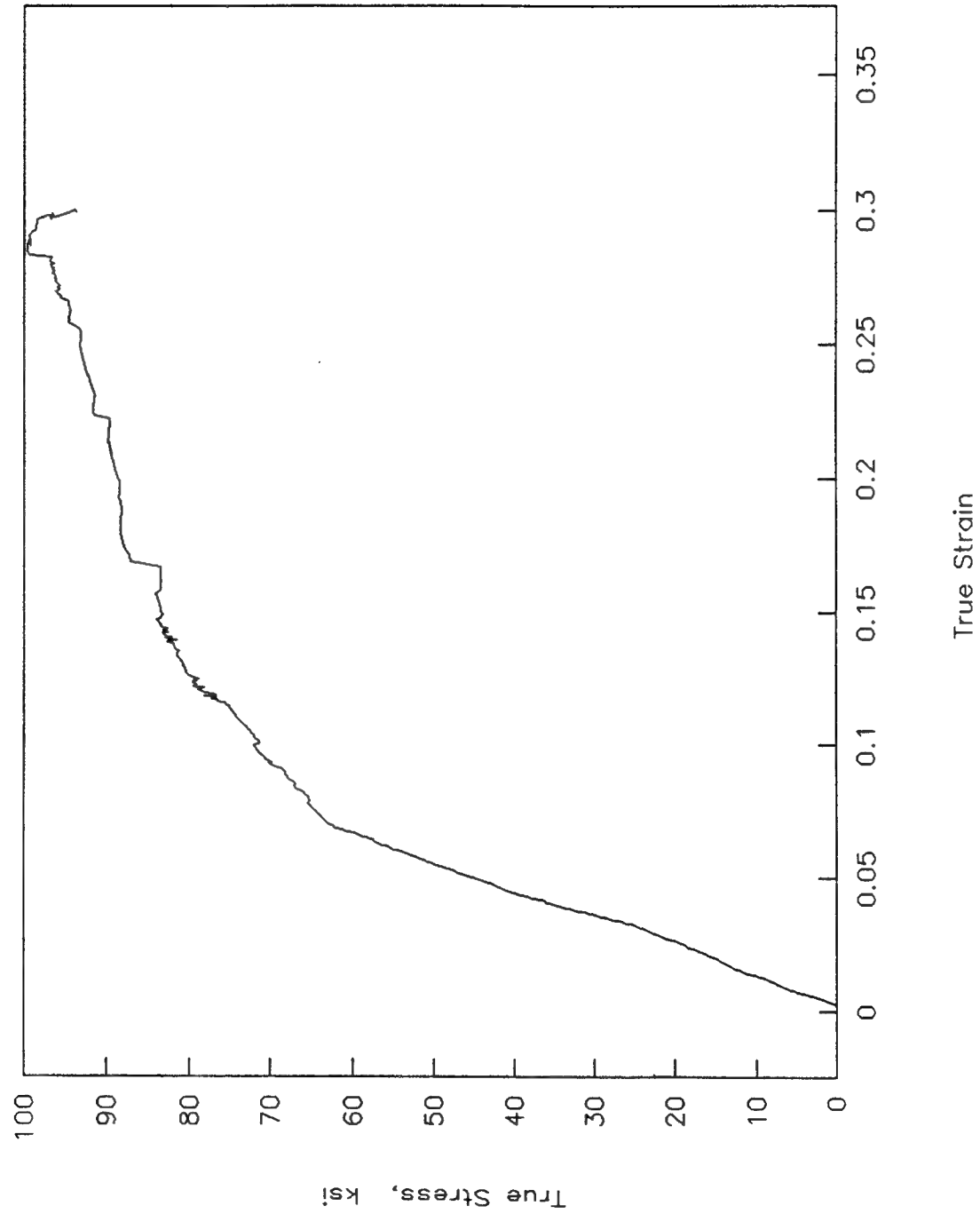


Figure 11. Stress - strain curve for specimen W1100-10 tested at 1100°F.

W1230-4
True Stress–True Strain (diametral)

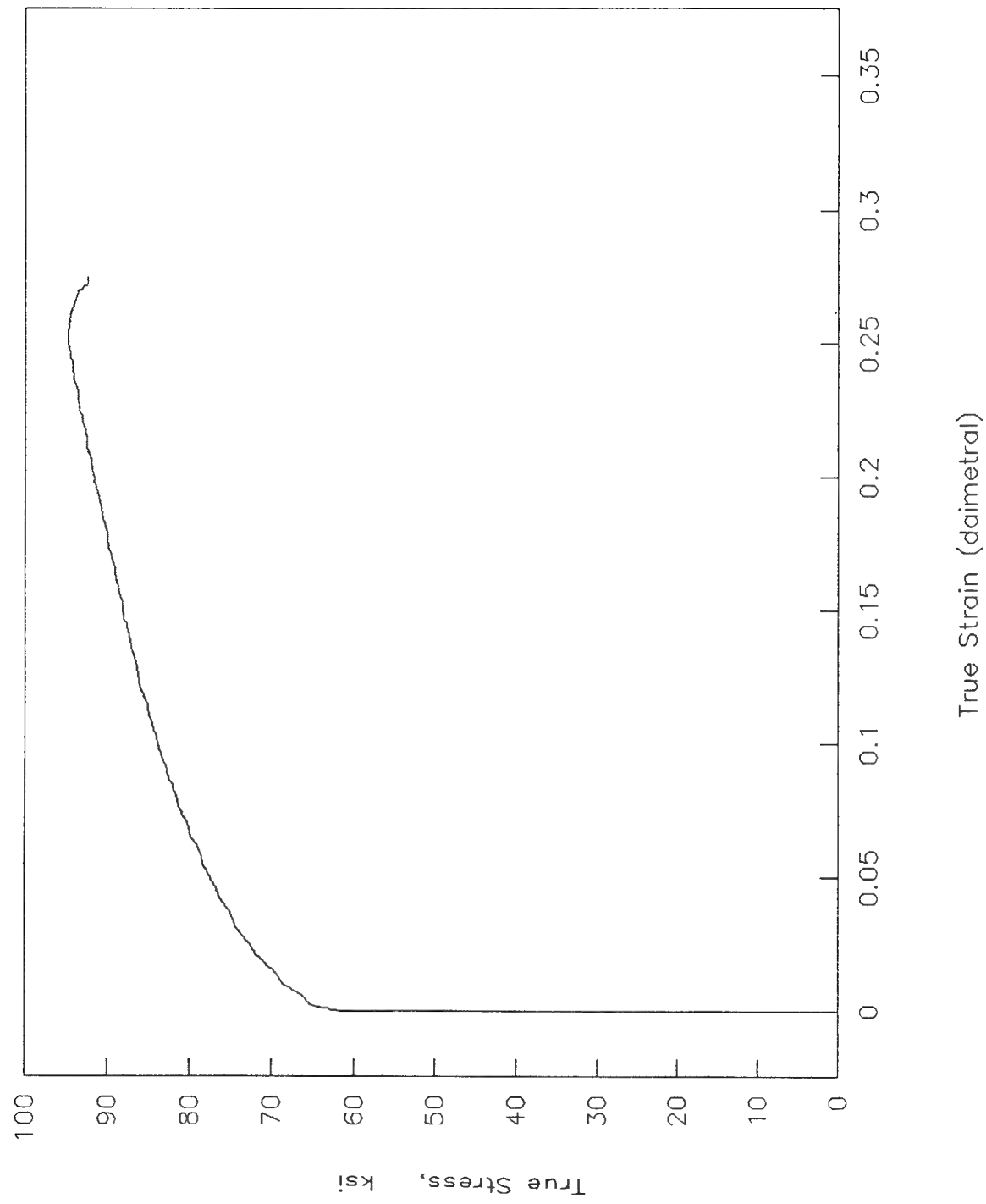


Figure 12. Stress – strain curve for specimen W1230-4 tested at 1230°F.

W1230-4

True Stress-True Strain (Longitudinal)

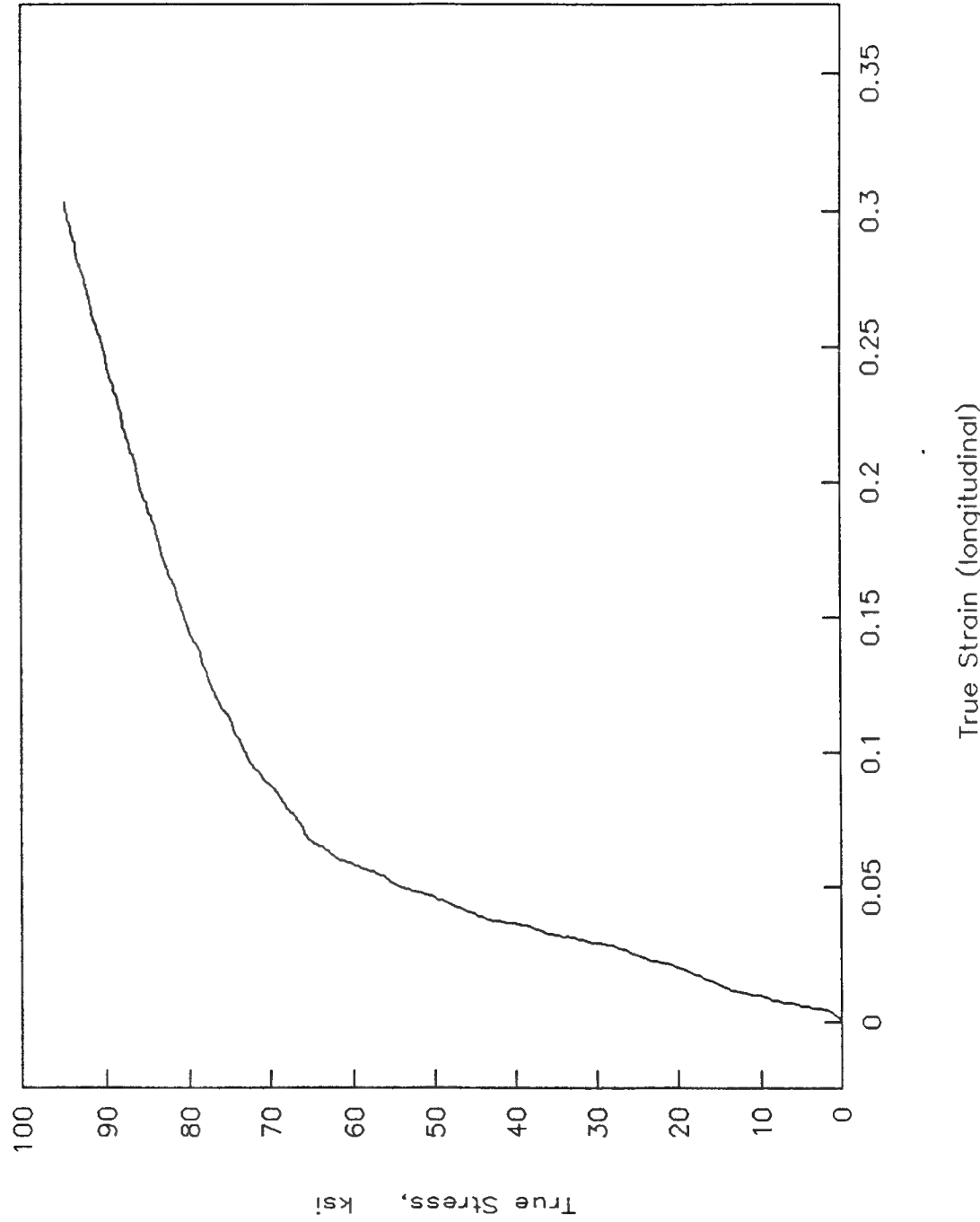


Figure 13. Stress - strain curve for specimen W1230-4 tested at 1230°F.

W1300-11
True Stress - True Strain (diametral)

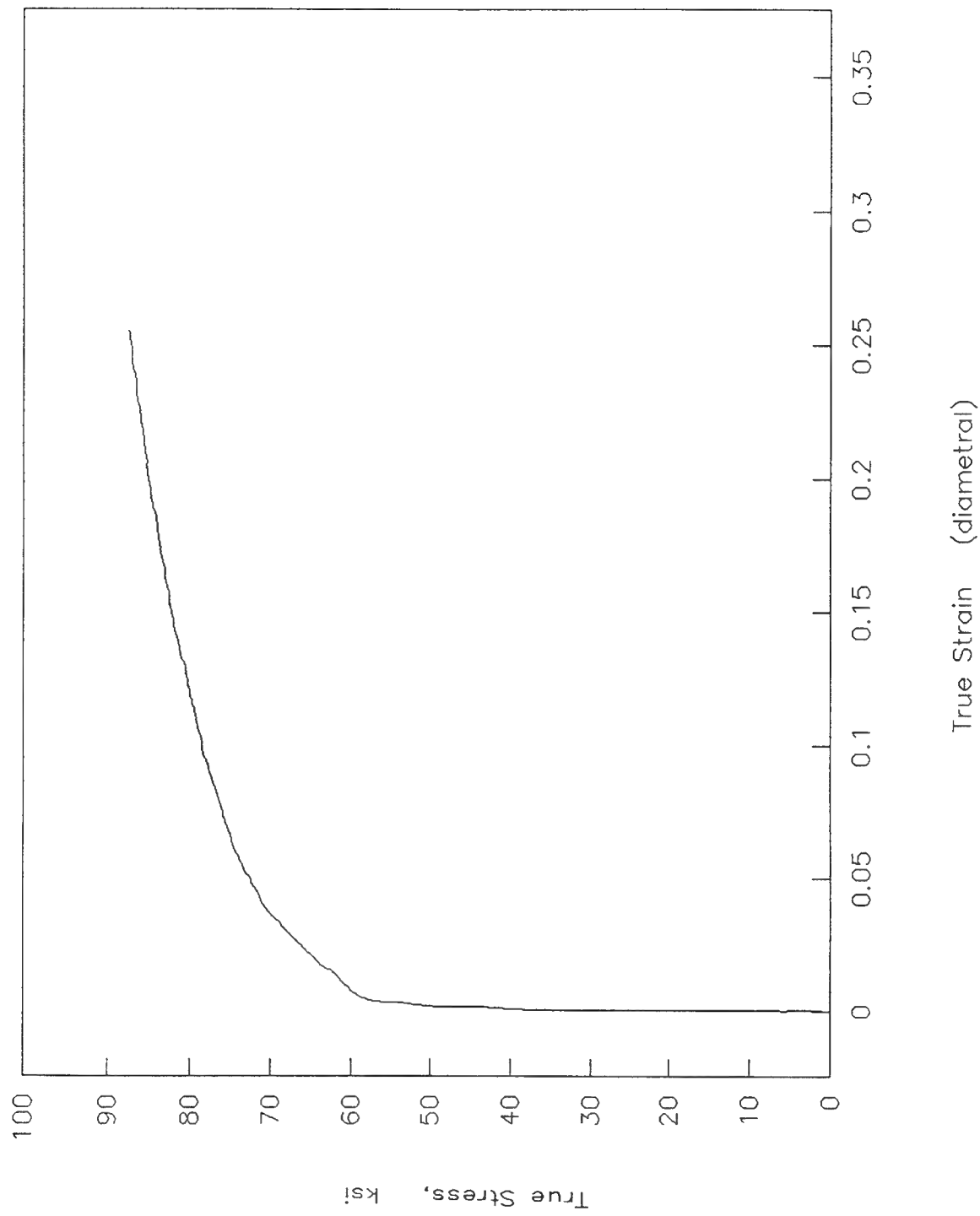


Figure 14. Stress - strain curve for specimen W1300-11 tested at 1300°F.

W1300-11

True Stress-True Strain (longitudinal)

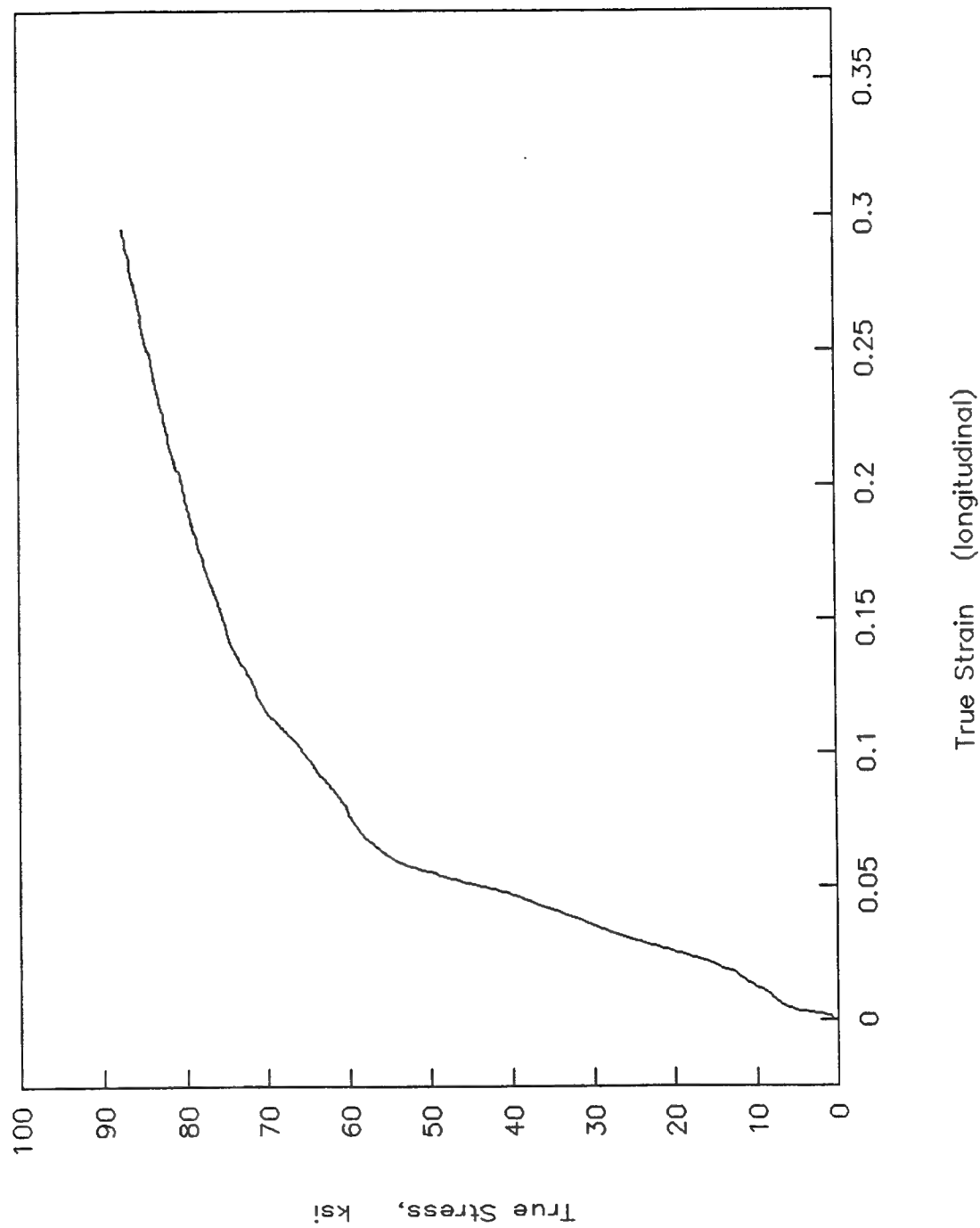


Figure 15. Stress - strain curve for specimen W1300-11 tested at 1300°F.

W1465-5

True Stress - True Strain (diametral)

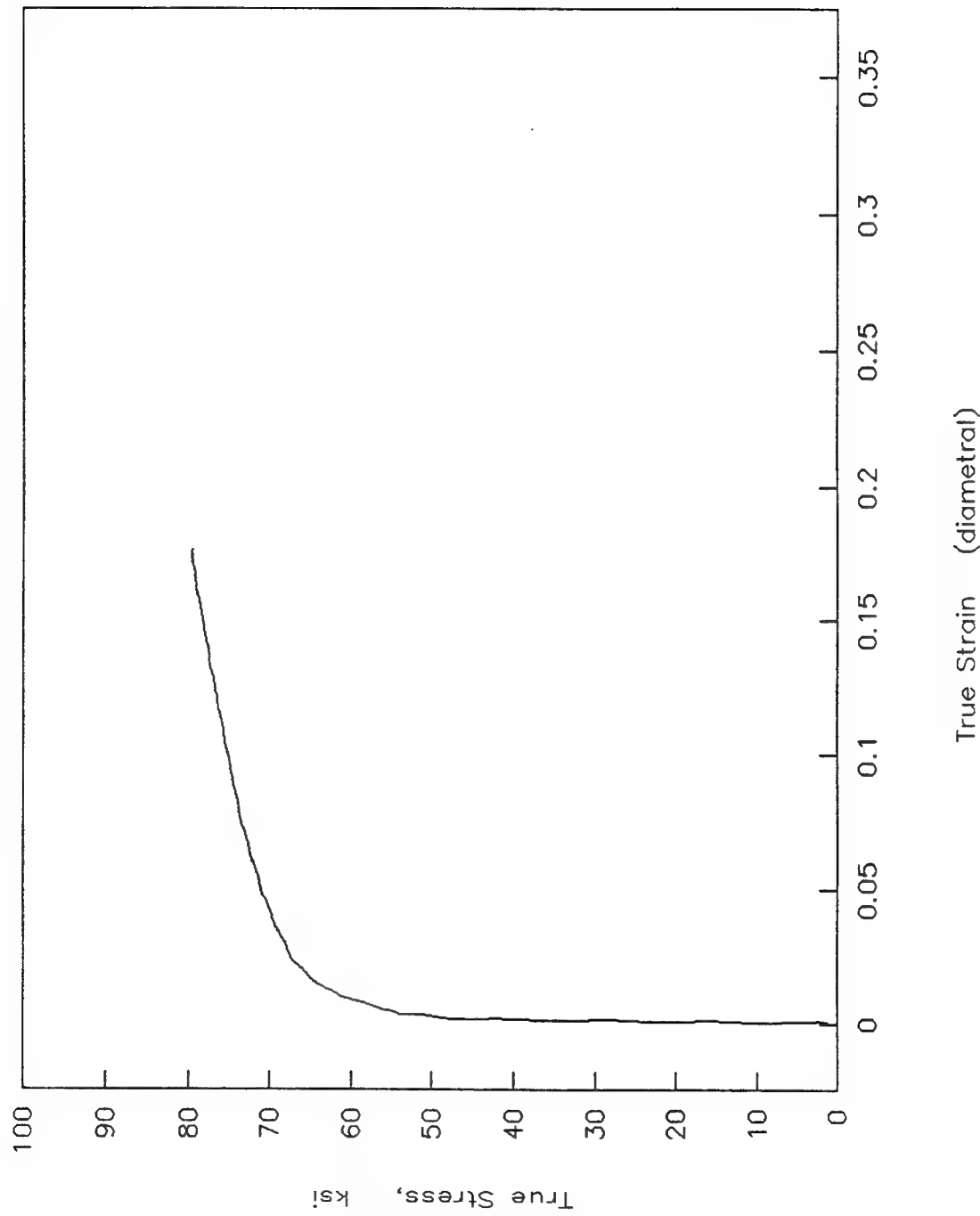


Figure 16. Stress - strain curve for specimen W1465-5 tested at 1465°F.

W1465-5

True Stress—True Strain (longitudinal)

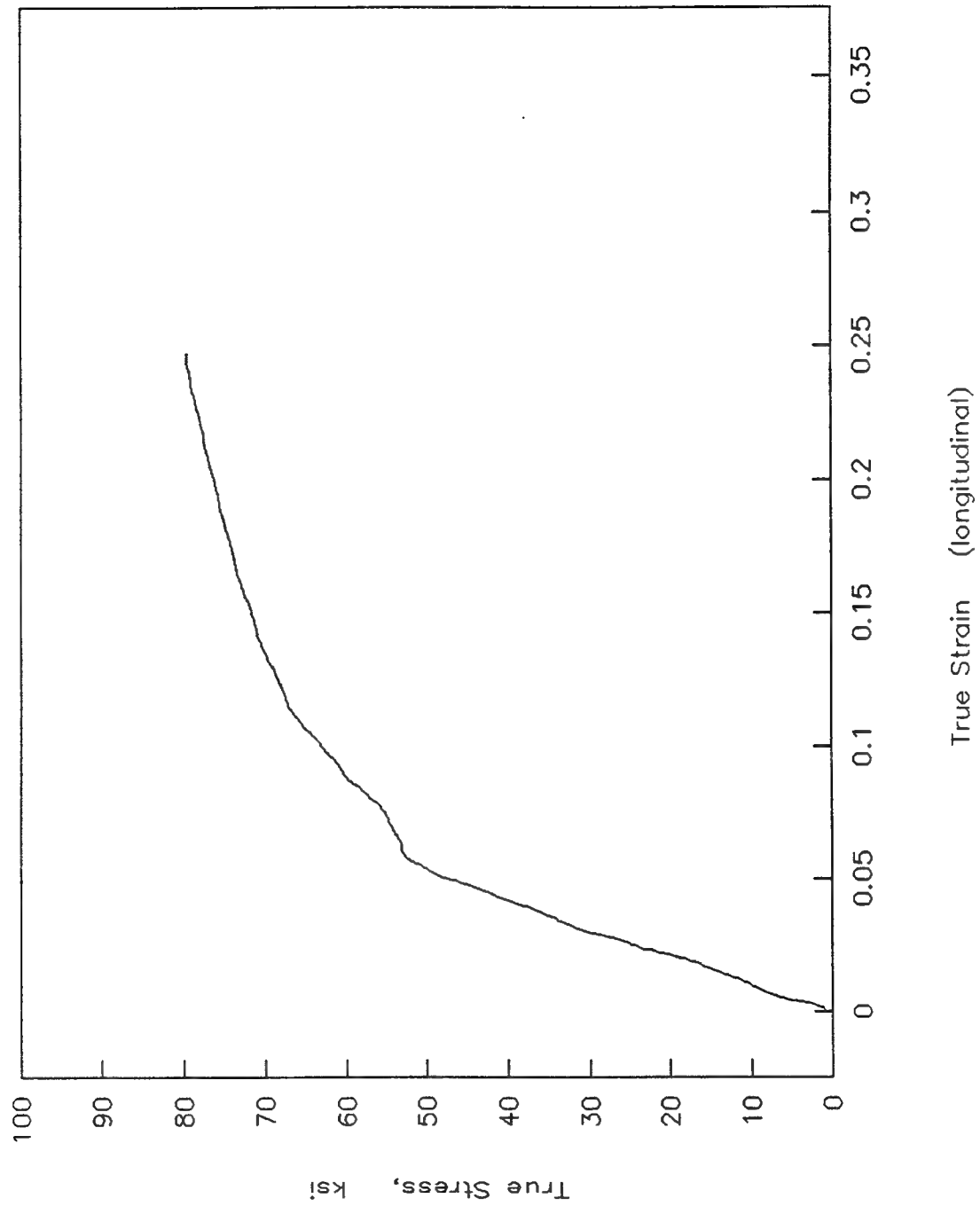


Figure 17. Stress - strain curve for specimen W1465-5 tested at 1465°F.

W1700-6

True Stress - True Strain (diametral)

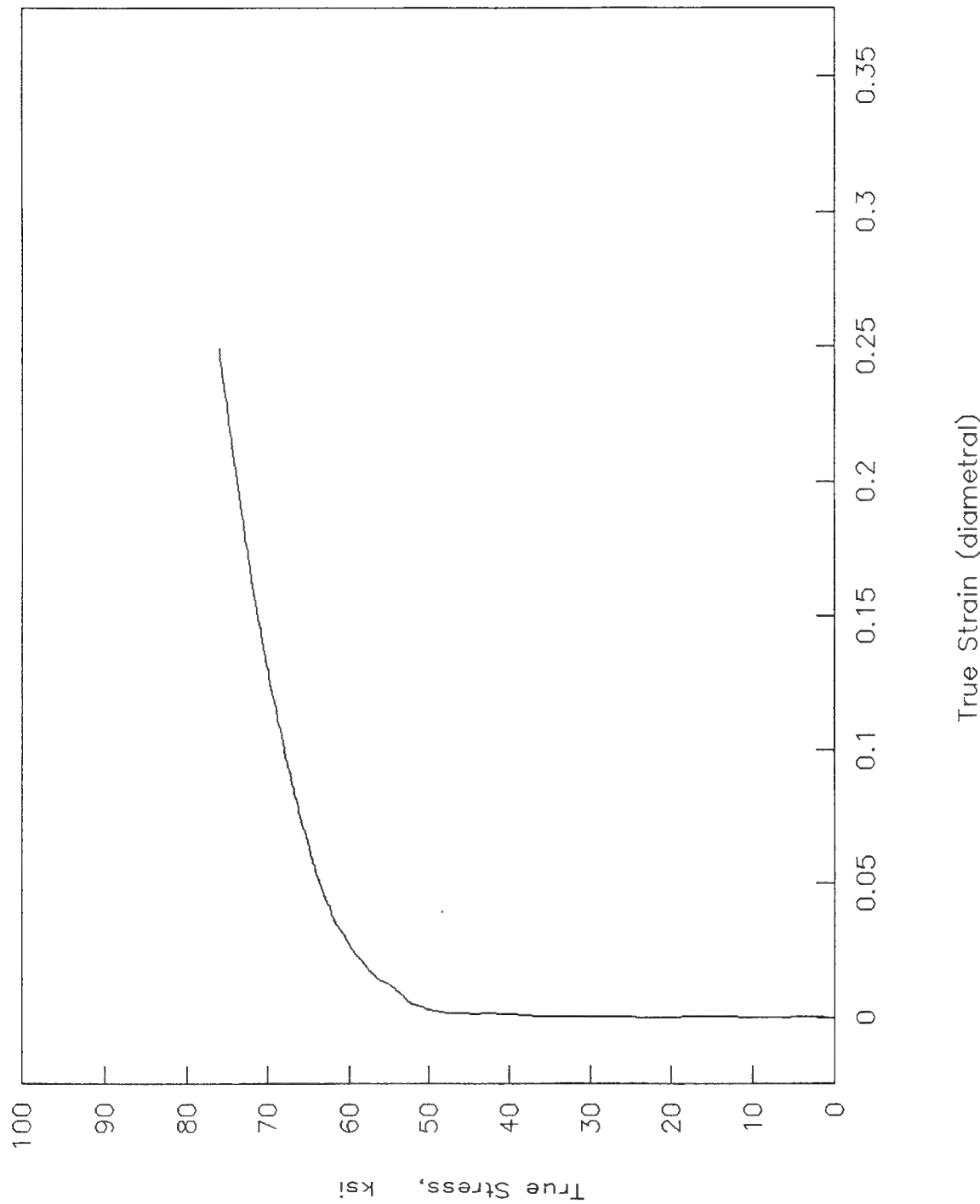


Figure 18. Stress - strain curve for specimen W1700-6 tested at 1700°F.

W1700-6

True Stress–True Strain (longitudinal)

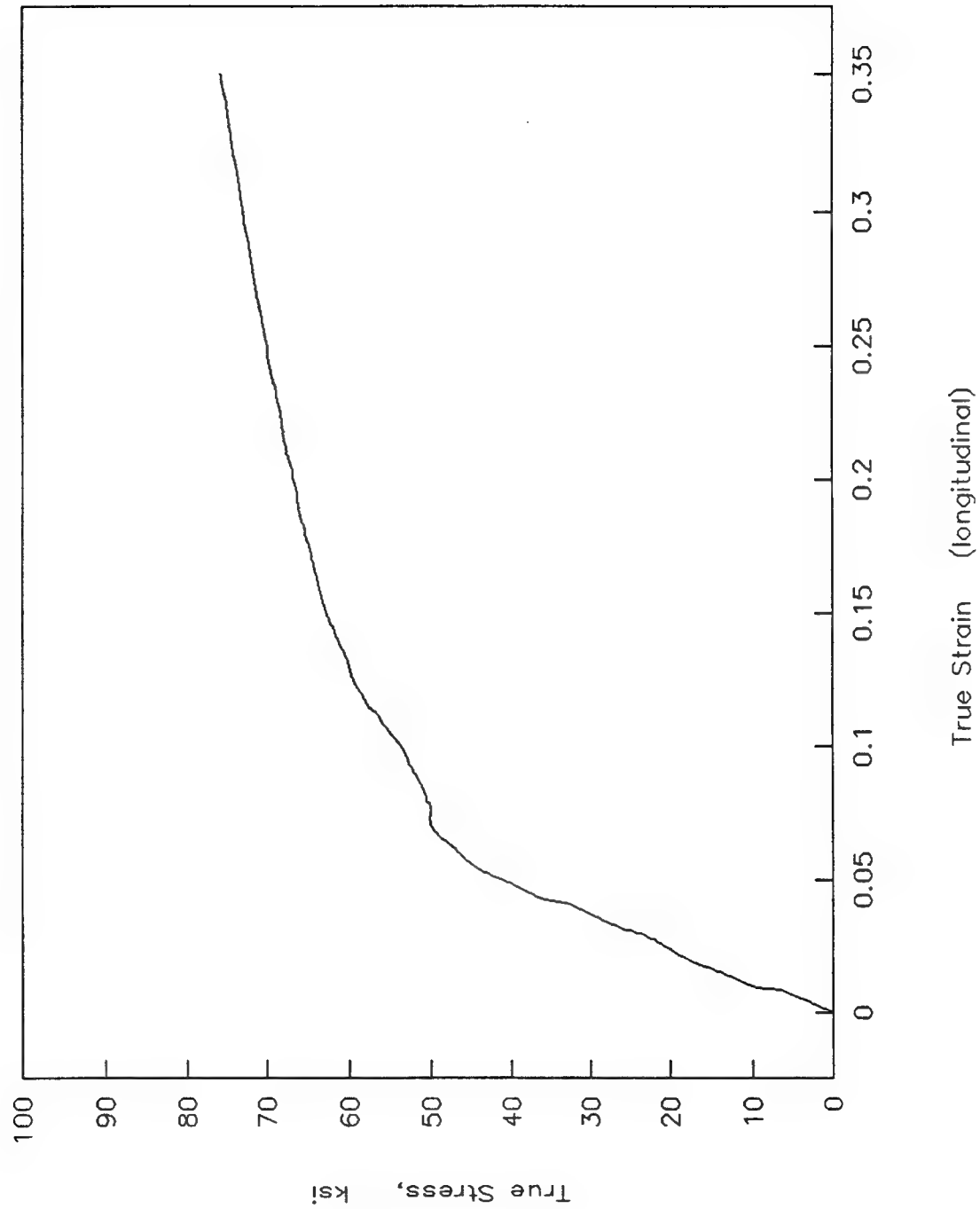


Figure 19. Stress – strain curve for specimen W1700-6 tested at 1700°F.

W1930-7

True Stress - True Strain (diametral)

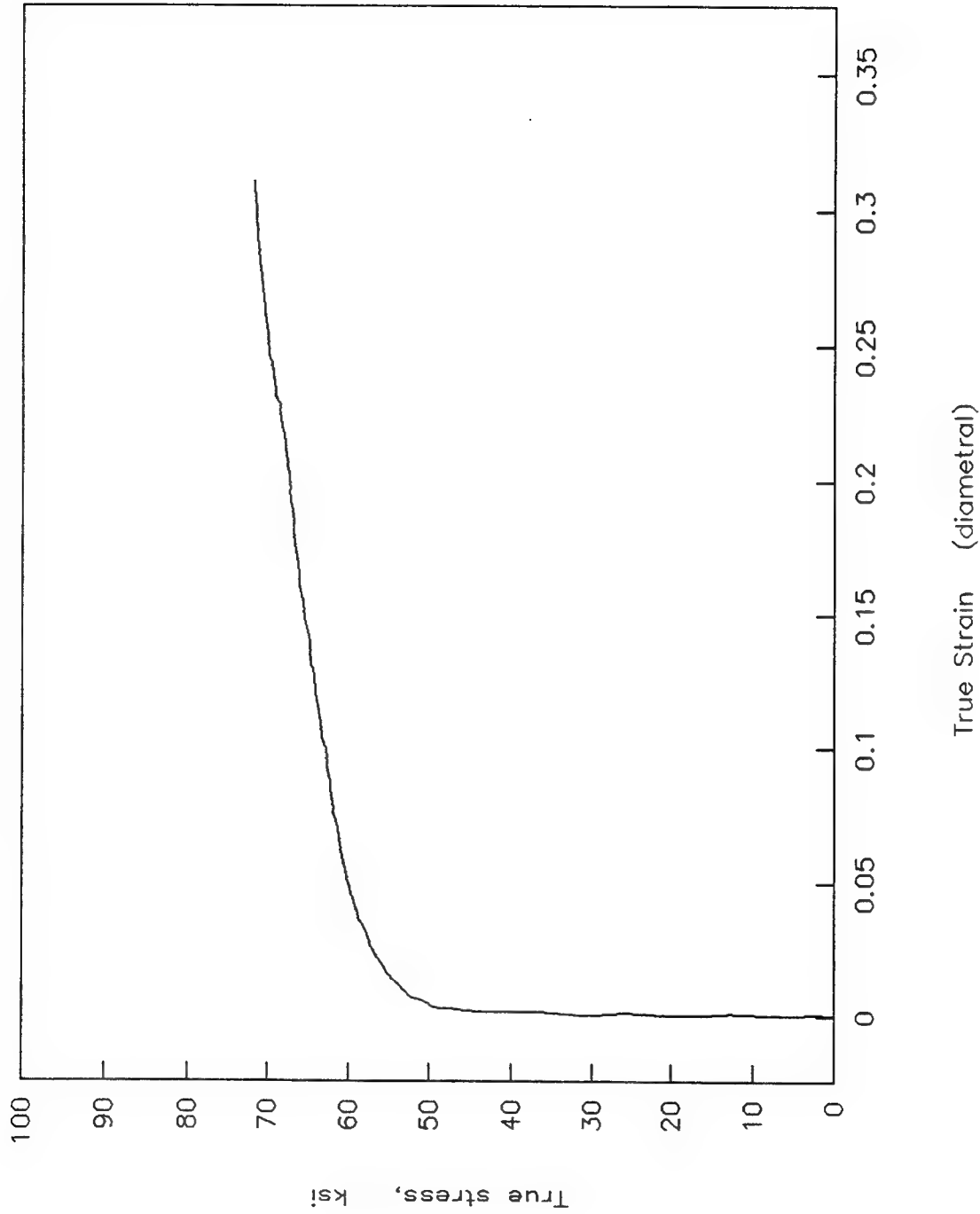


Figure 20. Stress - strain curve for specimen W1930-7 tested at 1930°F.

W1930-7

True Stress-True Strain (longitudinal)

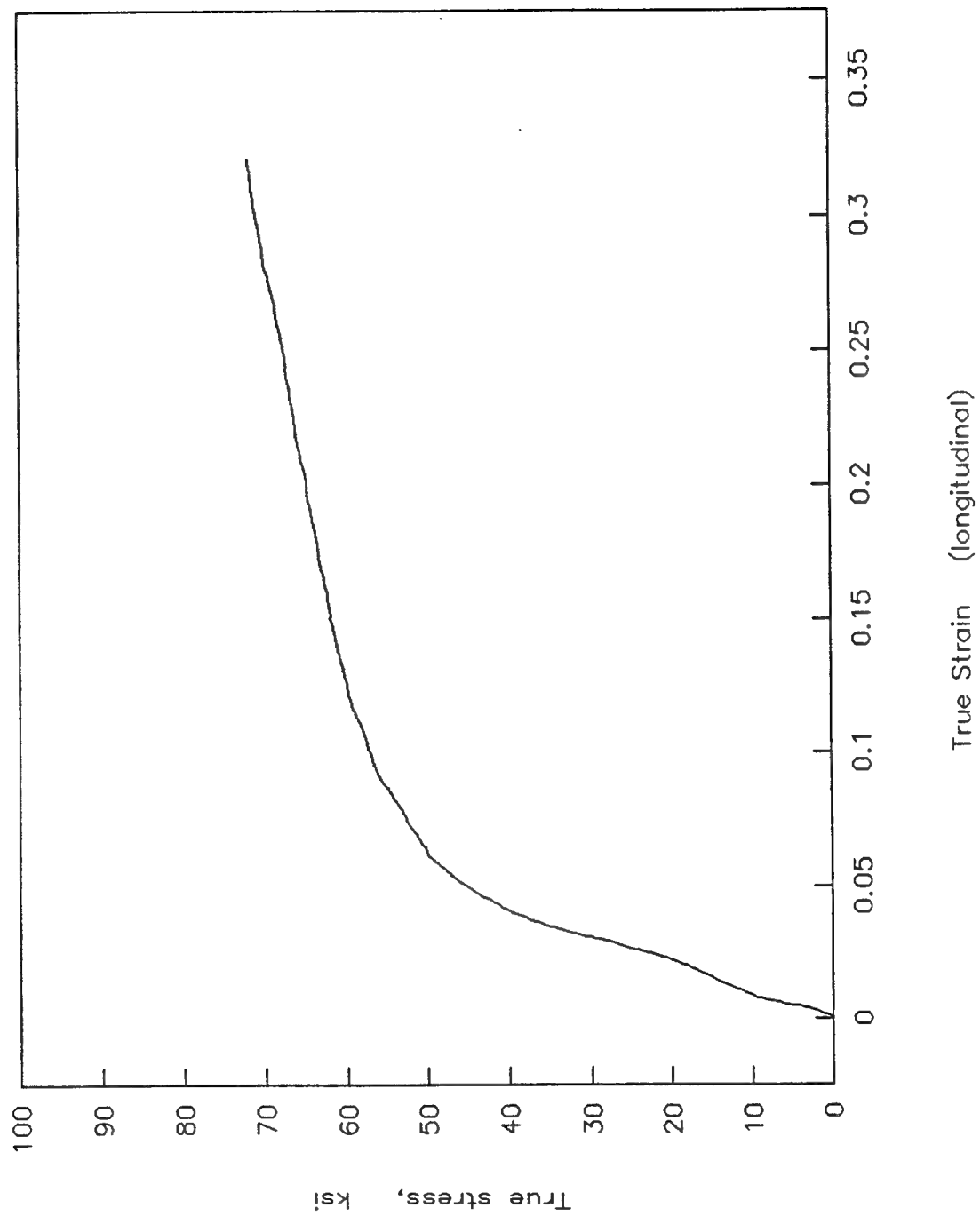


Figure 21. Stress - strain curve for specimen W1930-7 tested at 1930°F.

W1930 - 14 (Slow, 0.01 inch/sec.)
True stress - True Strain (diametral)

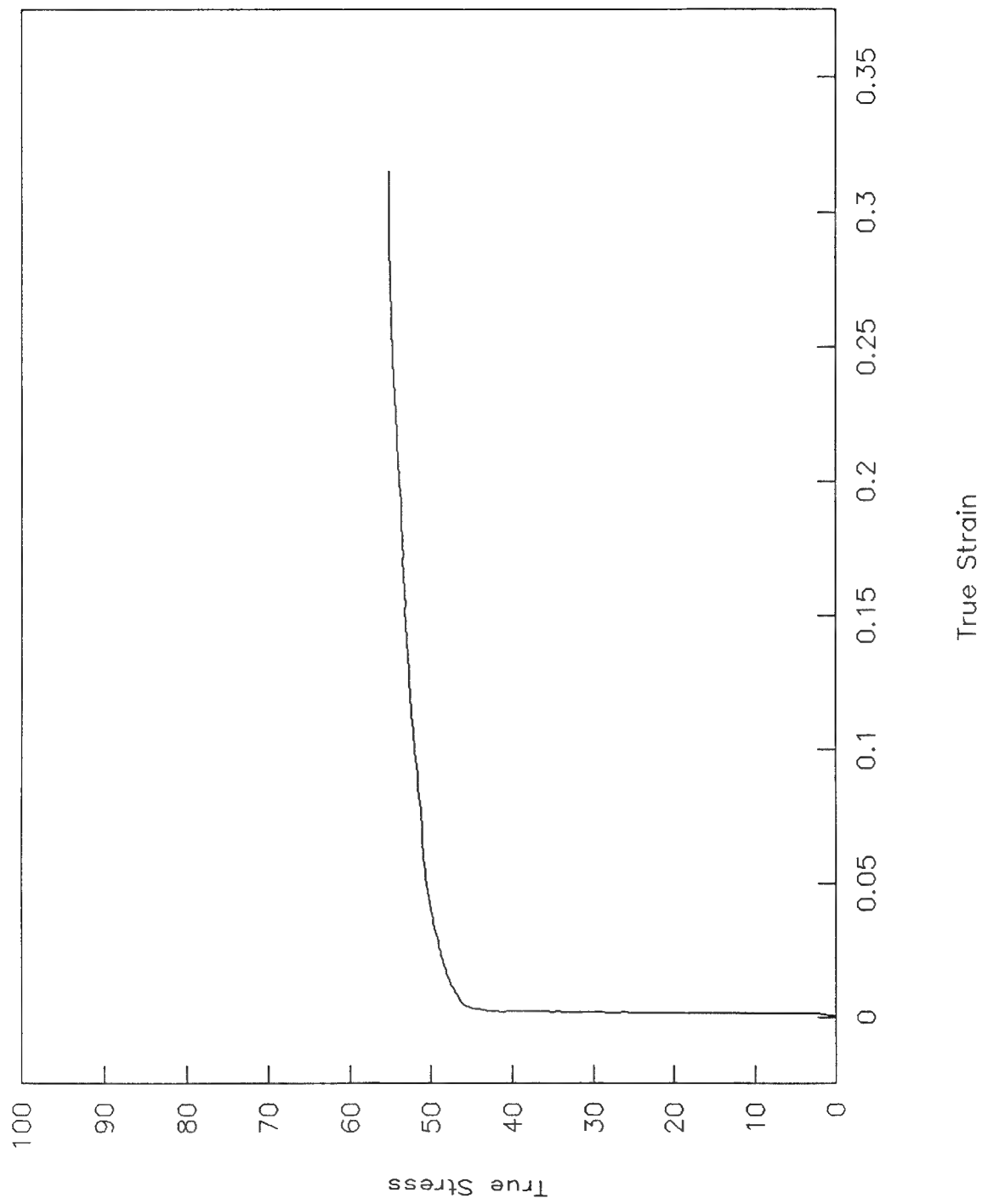


Figure 22. Stress - strain curve for specimen W1930-14 tested at 1930°F.

W1930-14 (slow, 0.01 inch/sec.)
True stress-True strain (longitudinal)

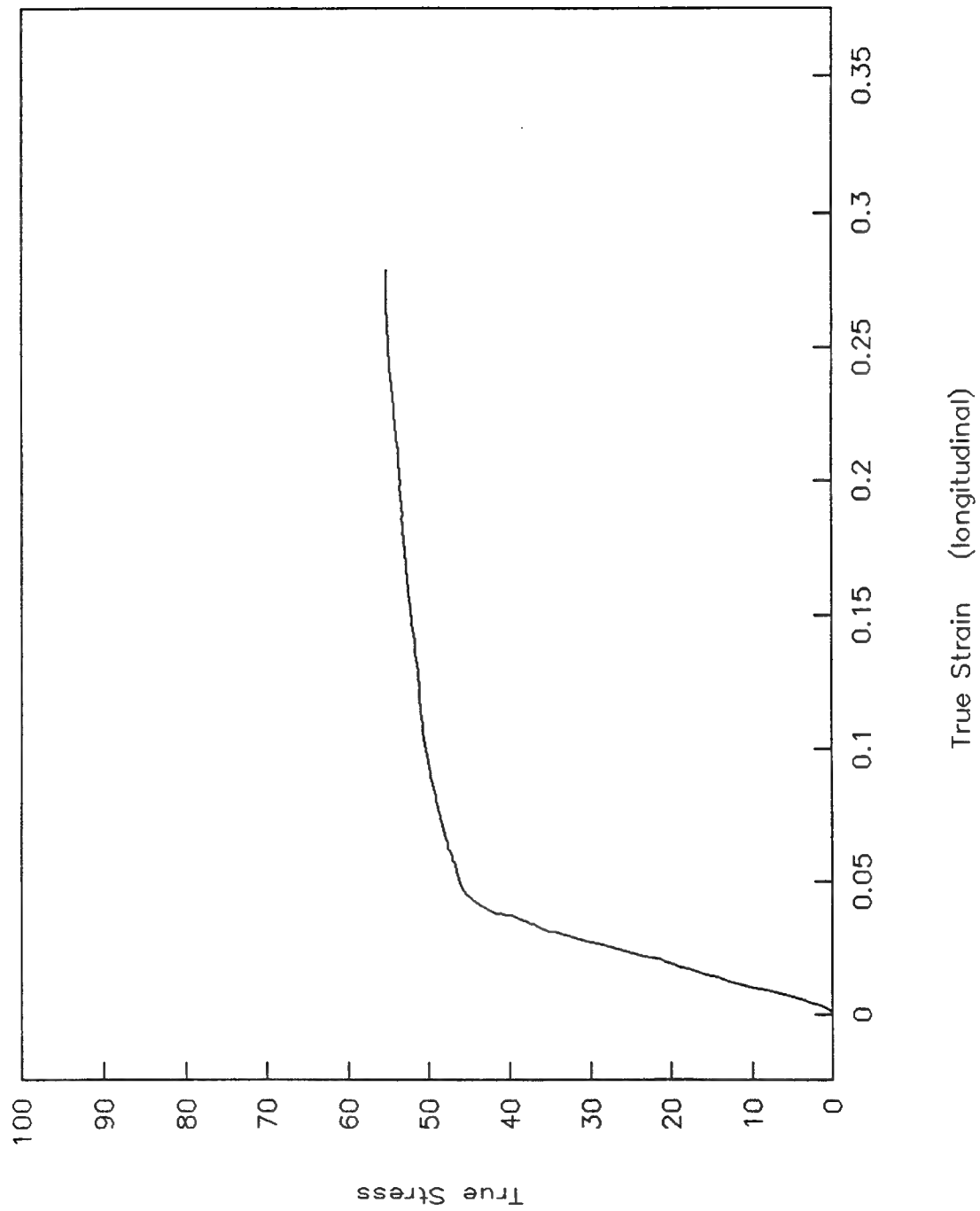


Figure 23. Stress - strain curve for specimen W1930-14 tested at 1930°F.

W2158-T1
True Stress - True Strain (diametral)

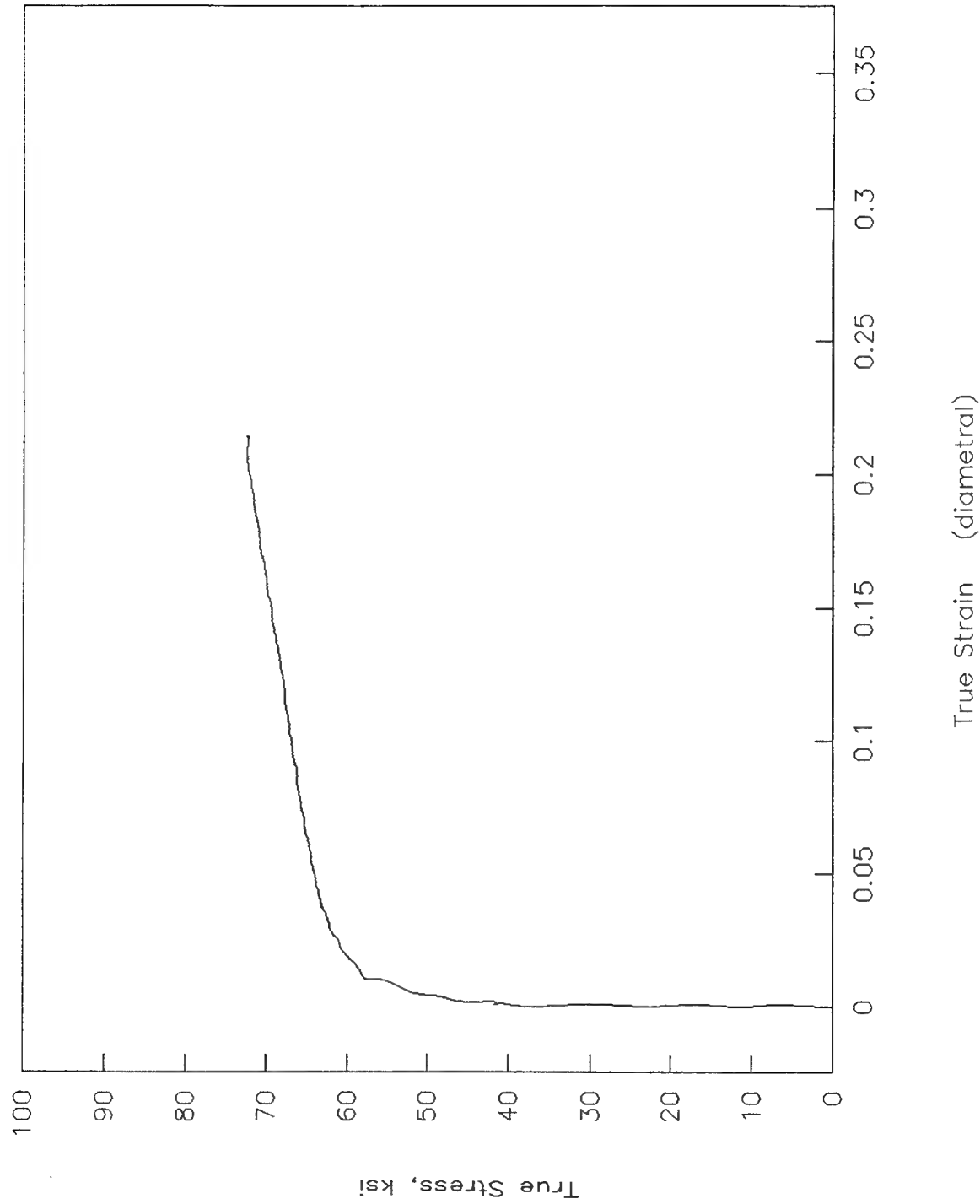


Figure 24. Stress - strain curve for specimen W2158-T1 tested at 2158°F.

W2158-T1

True stress-True strain (longitudinal)

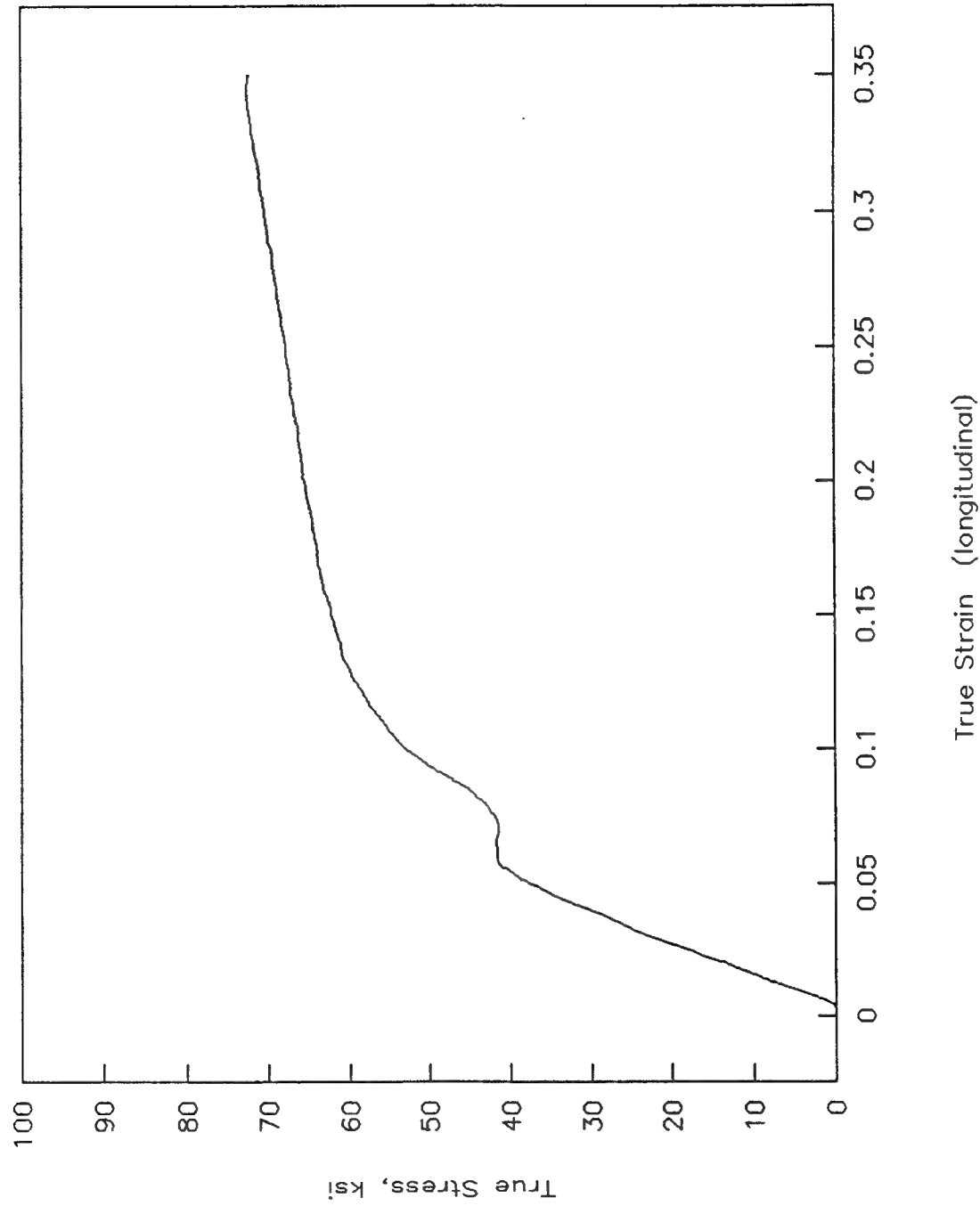


Figure 25. Stress - strain curve for specimen W2158-T1 tested at 2158°F.

W2158-T2

True stress – True strain (diametral)

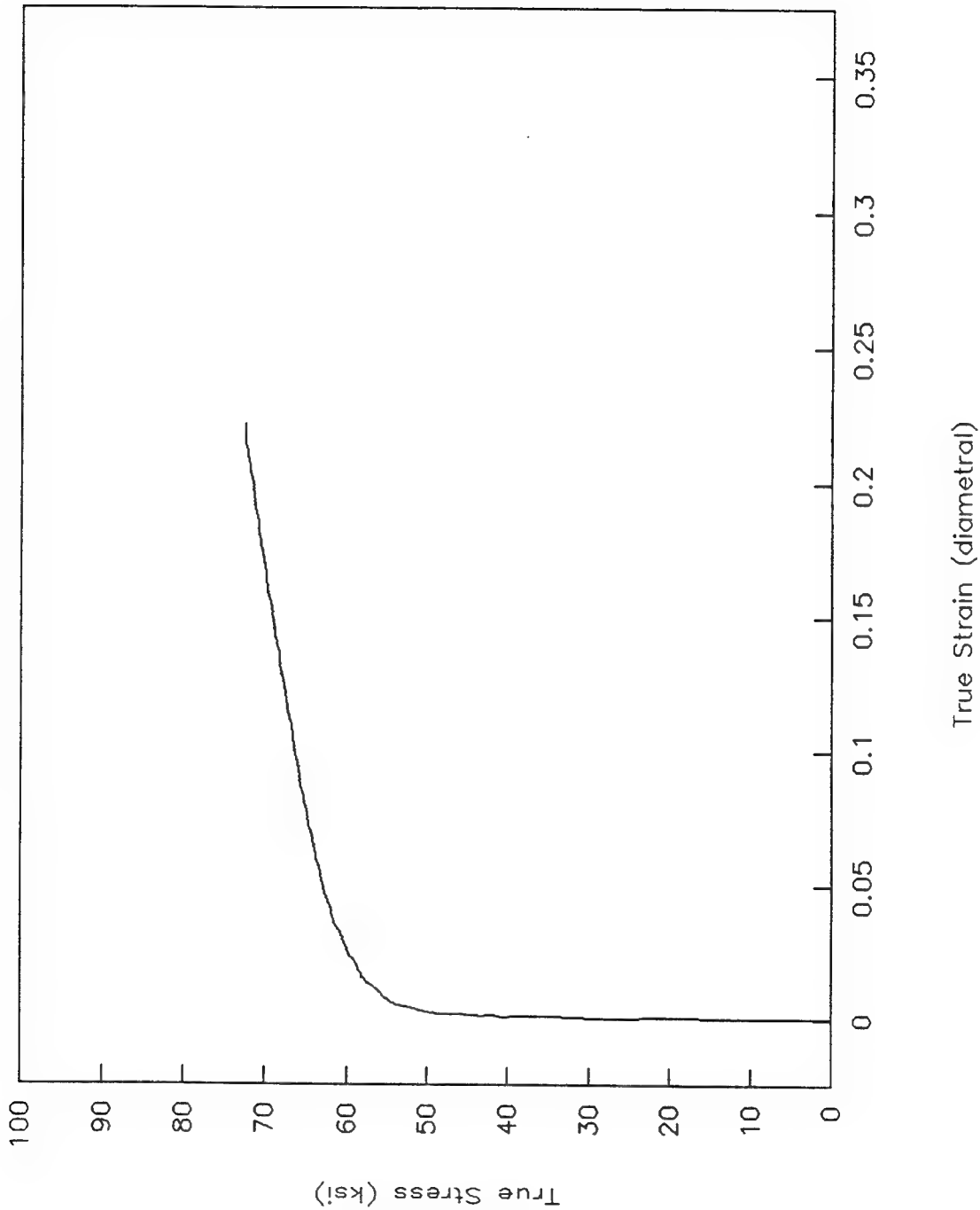


Figure 26. Stress – strain curve for specimen W2158-T2 tested at 2158°F.

W2158-T2

True stress-True strain (longitudinal)

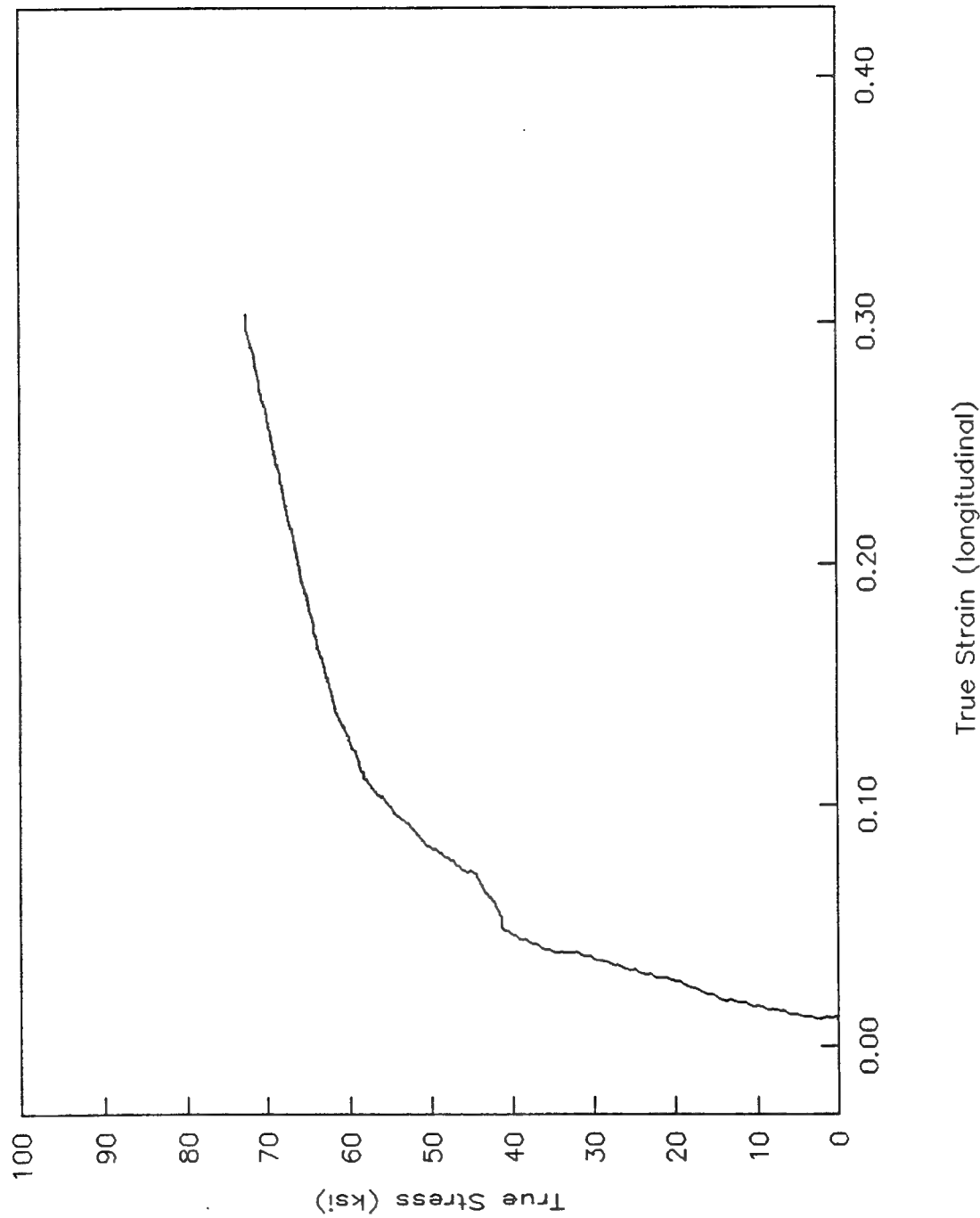


Figure 27. Stress - strain curve for specimen W2158-T2 tested at 2158°F.

W2400-2

True Stress - True Strain (diametral)

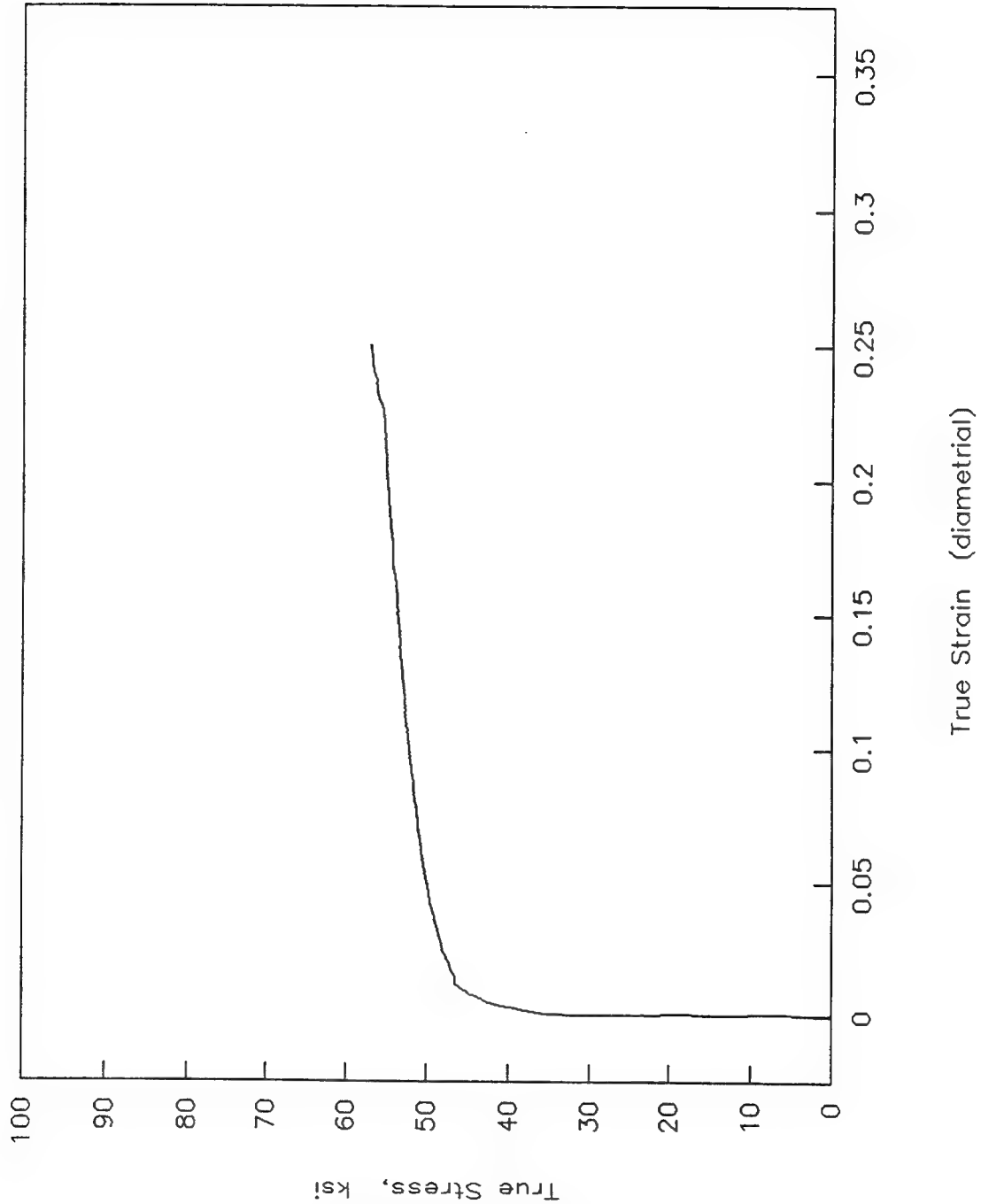


Figure 28. Stress - strain curve for specimen W2400-2 tested at 2400°F.

W2400-2

True Stress-True Strain (longitudinal)

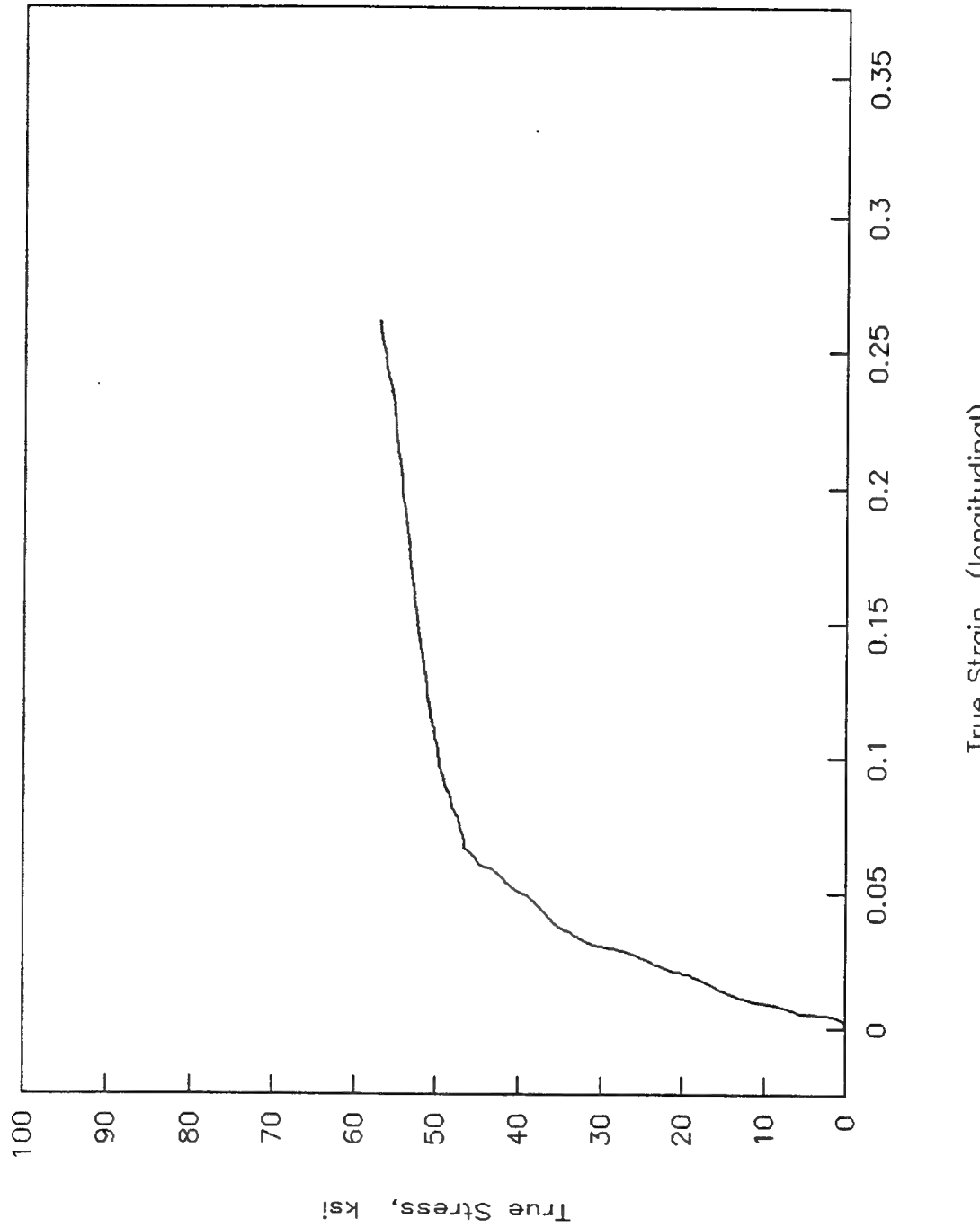


Figure 29. Stress - strain curve for specimen W2400-2 tested at 2400°F.

W3000-12

True stress - True strain (diametral)

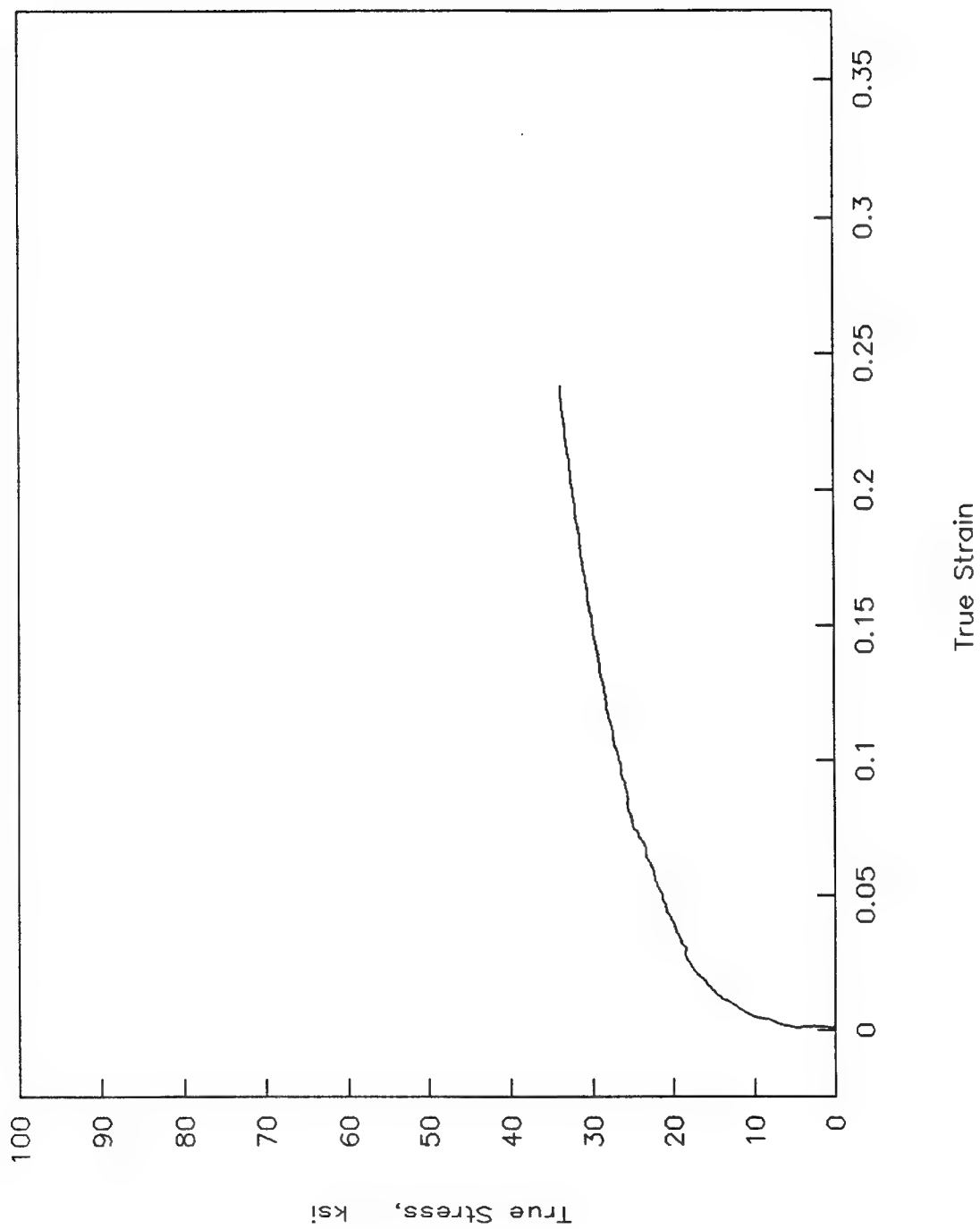


Figure 30. Stress - strain curve for specimen W3000-12 tested at 3000°F.

W3000-12

True stress—True strain (longitudinal)

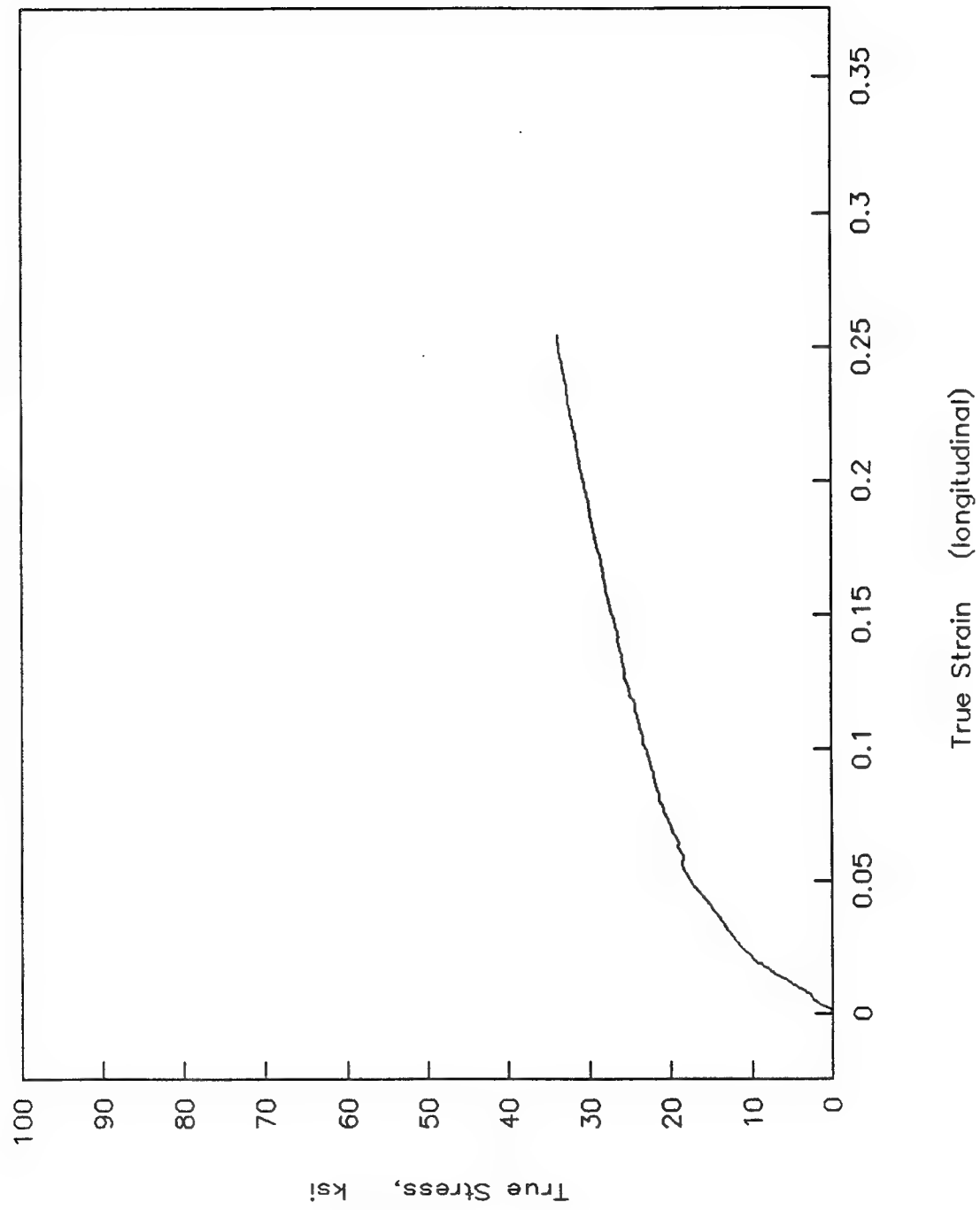


Figure 31. Stress - strain curve for specimen W3000-12 tested at 3000°F.

0.2% Offset Yield Strength for Tungsten
versus Temperature

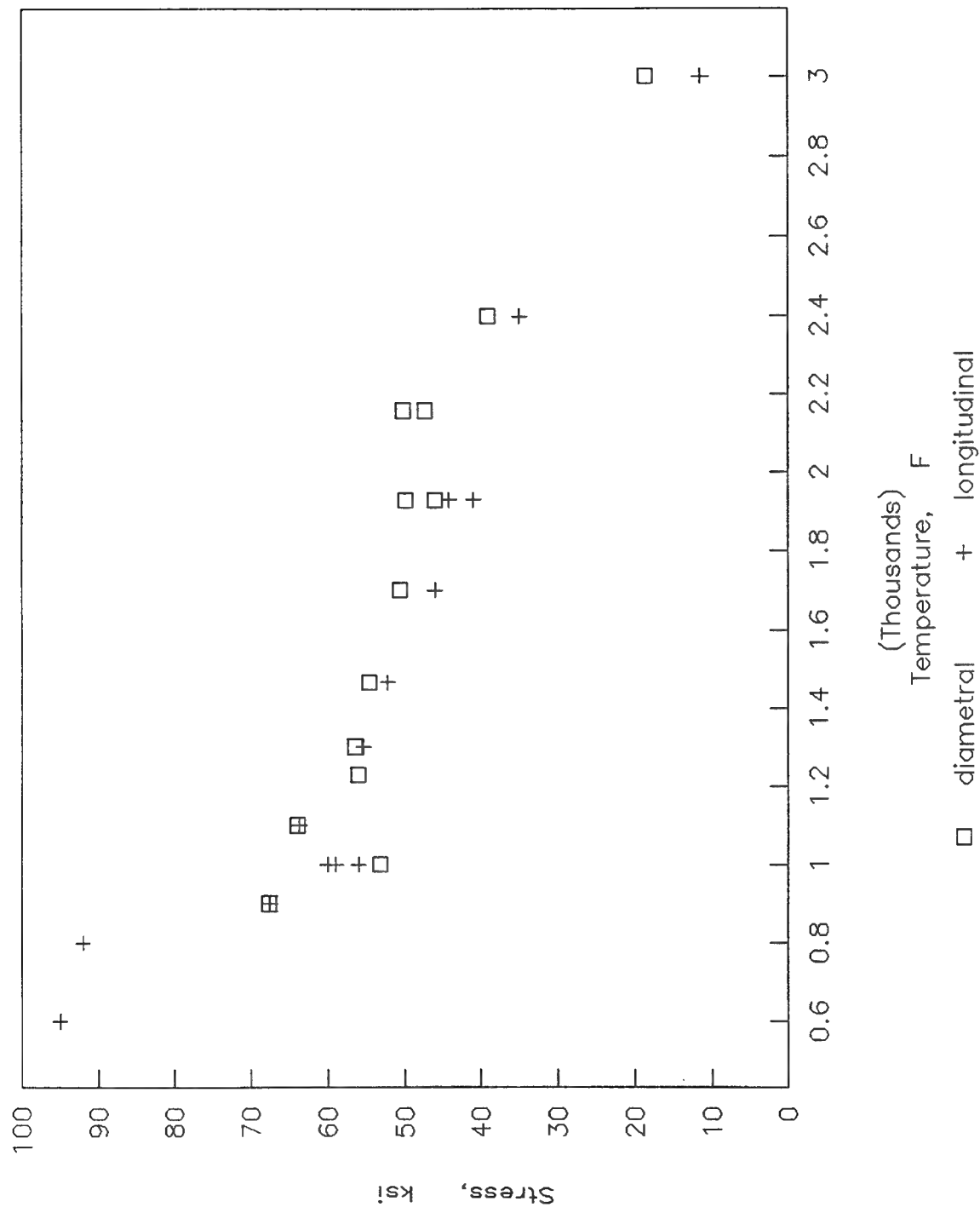


Figure 32. 0.2% offset yield strength for tungsten tested at 600 to 3000°F.

5.0% Offset Yield Strength for Tungsten
versus Temperature

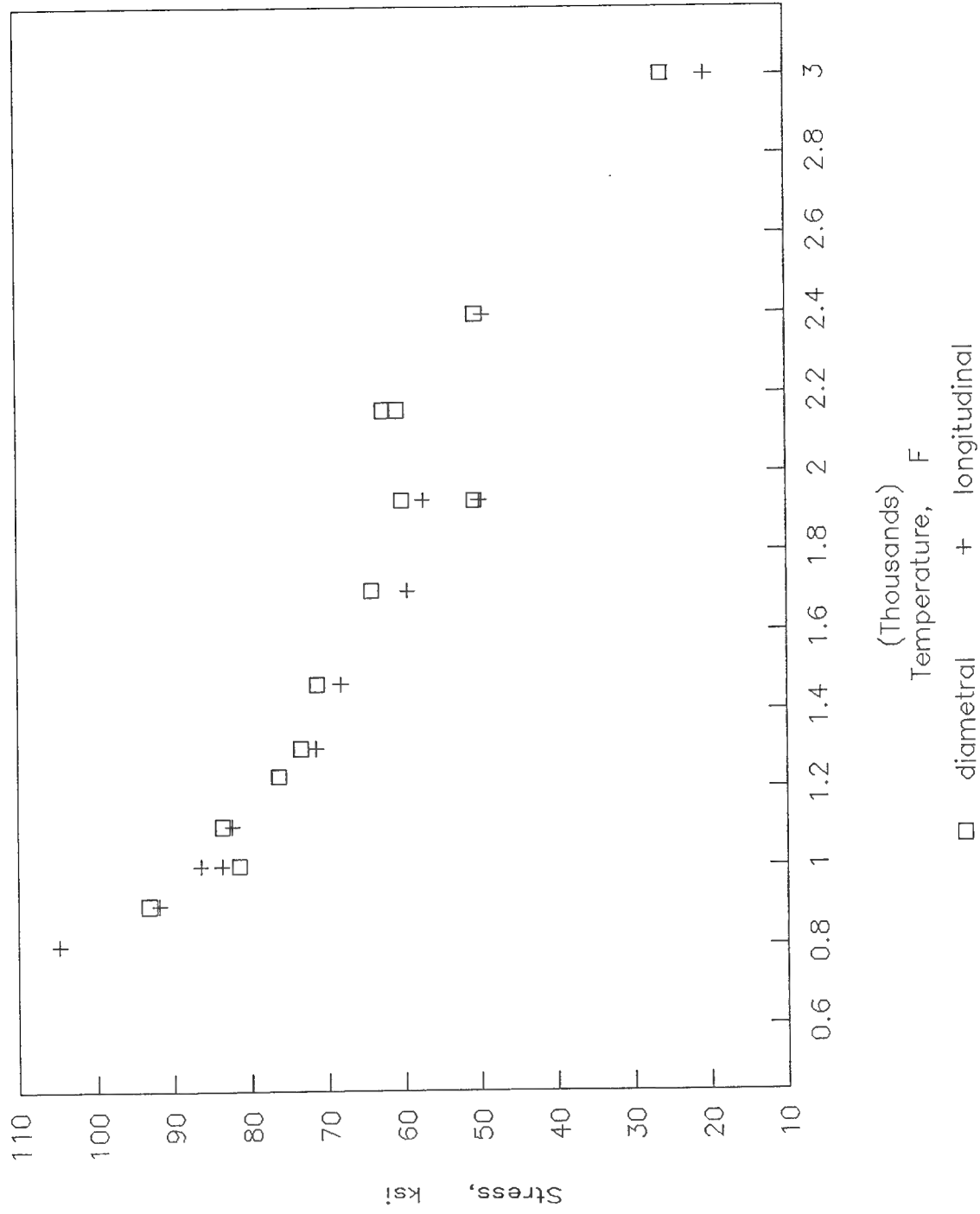


Figure 33. 5.0% offset yield strength for tungsten tested at 600 to 3000°F.

Anisotropy of Tungsten
R (max/min diameter) vs. Temperature

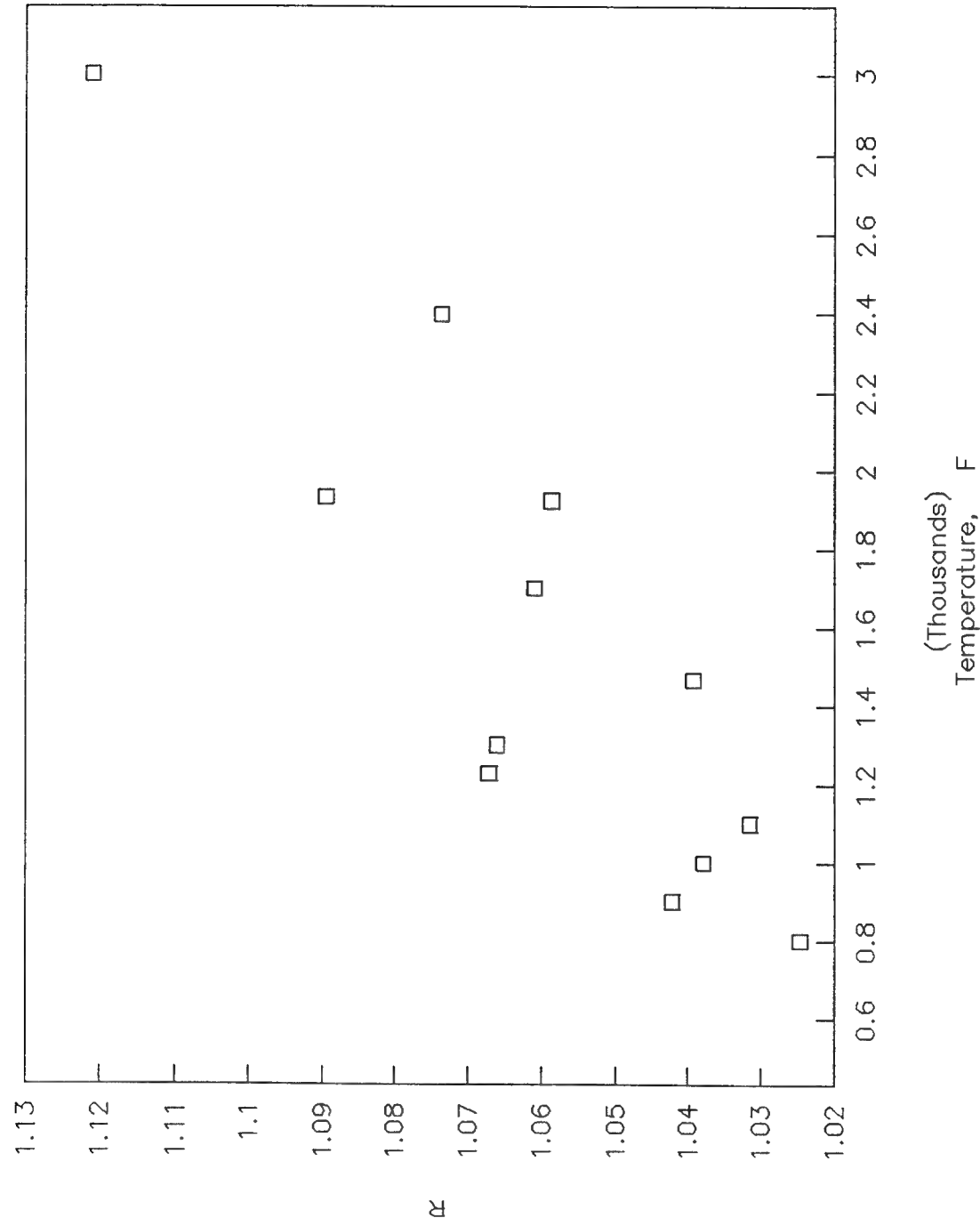
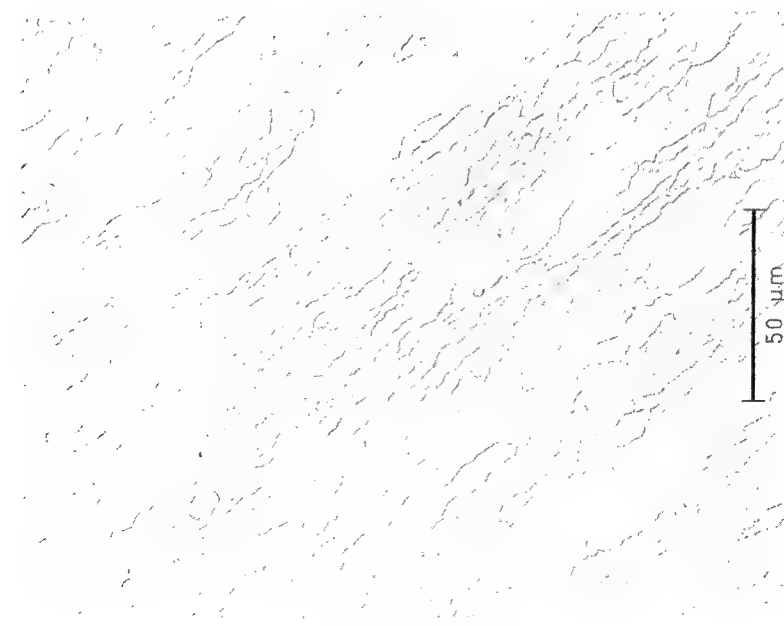


Figure 34. Plastic anisotropy "R" value for tungsten tested at 600 to 3000°F.



50X

Orientation to outer surface of liner



500X

Figure 35. Photomicrographs of tungsten in "as received" condition.



500 μ m

50X

Orientation to outer surface of liner



50 μ m

500X

Figure 36. Photomicrographs of tungsten specimen tested at 600°F.



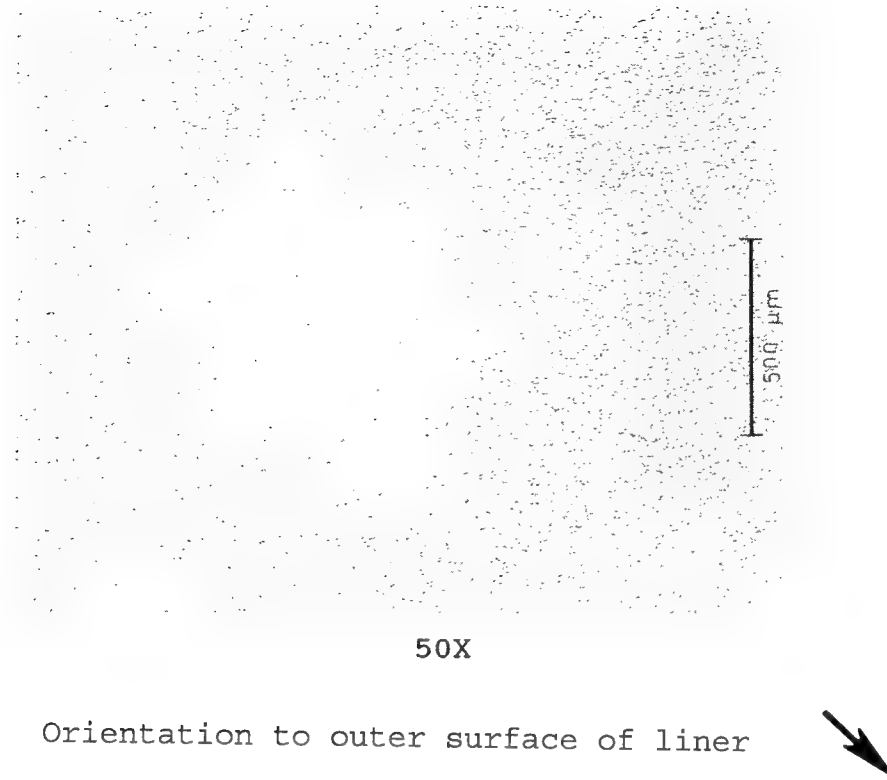
50X

Orientation to outer surface of liner



500X

Figure 37. Photomicrographs of tungsten specimen tested at 1700°F.



Orientation to outer surface of liner



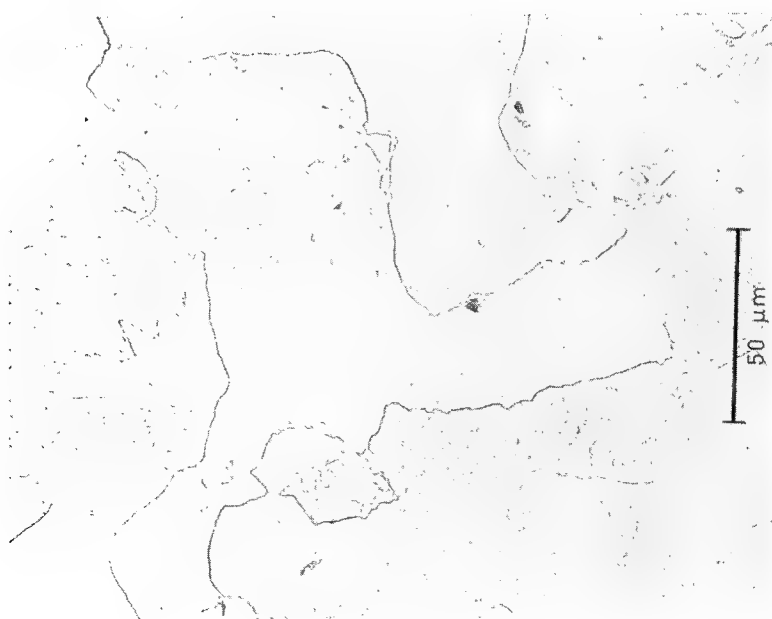
500X

Figure 38. Photomicrographs of tungsten specimen tested at 2400°F.



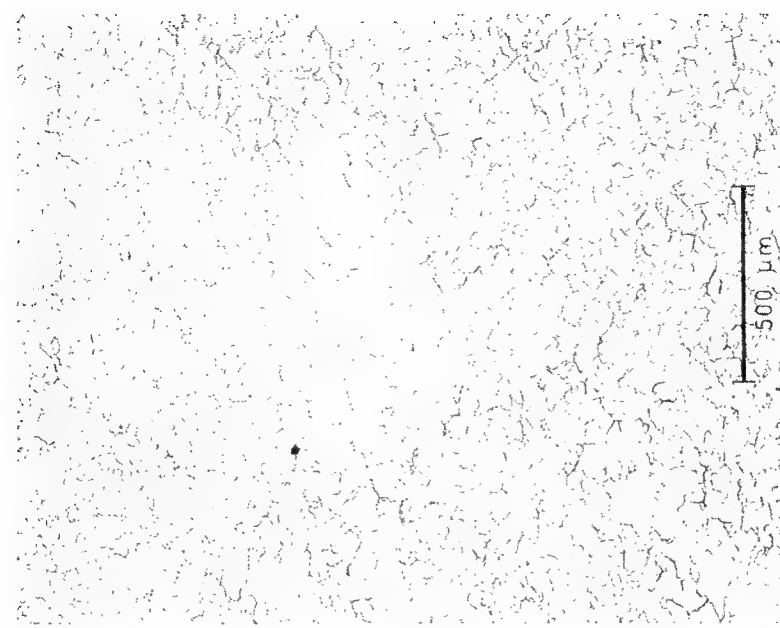
50X

Orientation to outer surface of liner



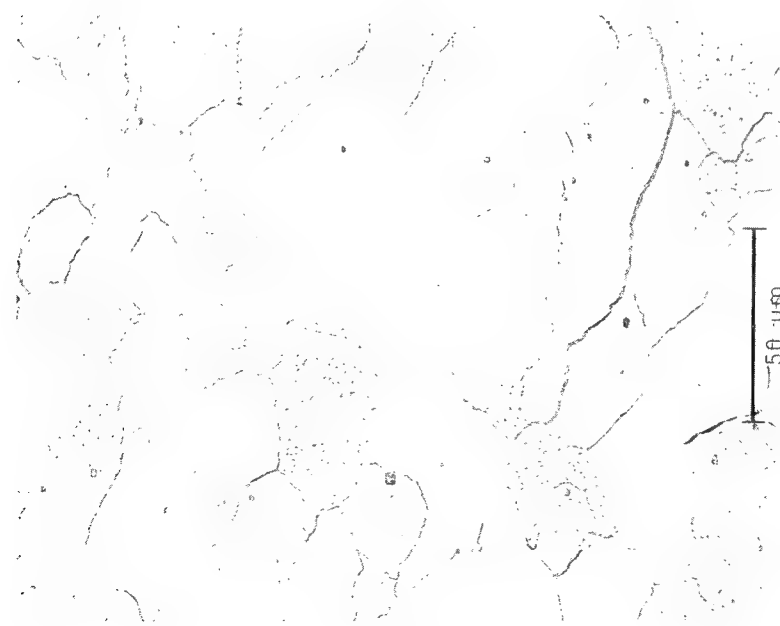
500X

Figure 39. Photomicrographs of tungsten specimen tested at 3000°F.



50X

Direction of longitudinal axis of specimen <----->

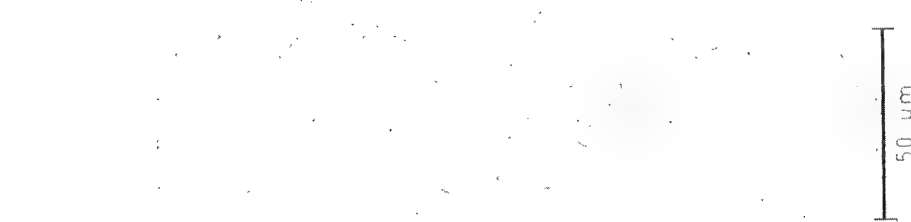


500X

Figure 40. Photomicrographs of tungsten specimen tested at 3000°F (longitudinal section) W3000-12



50X
Direction of longitudinal axis of specimen <----->



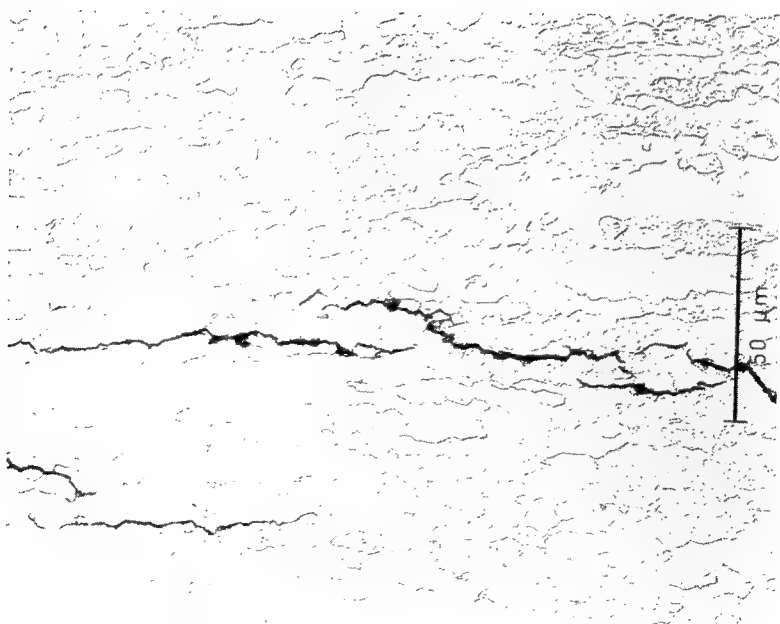
500X

Figure 41. Photomicrographs of tungsten specimen tested at 1100°F
(longitudinal section) W1100-10



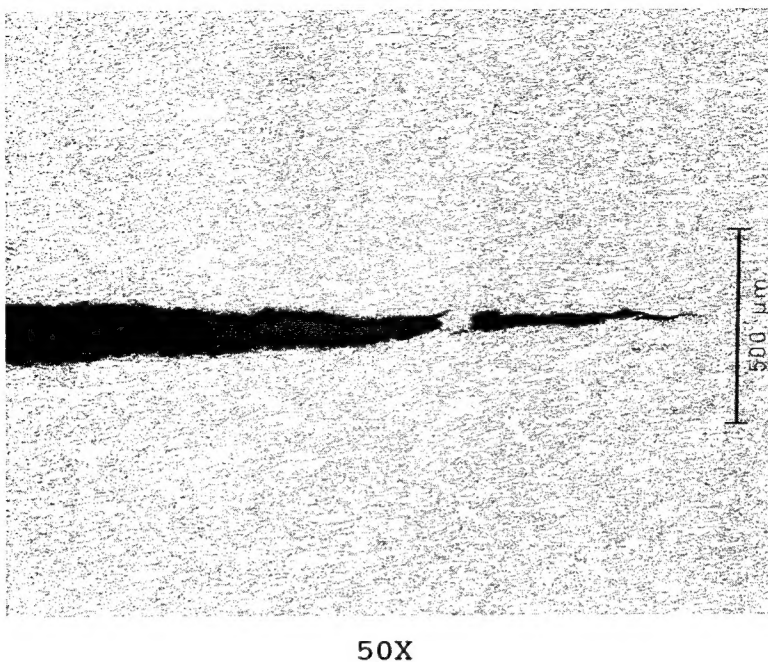
50X

Orientation to outer surface of liner



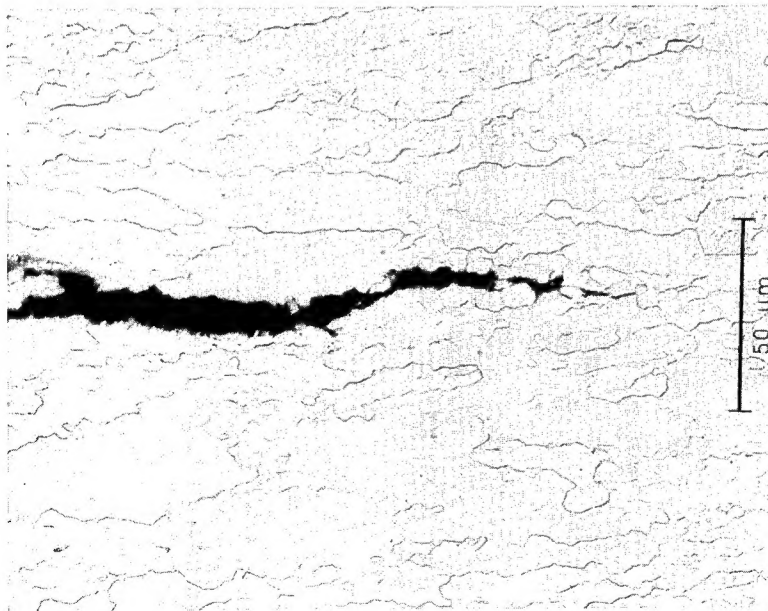
500X

Figure 42. Photomicrographs of crack in tungsten specimen W600-1 tested at 600°F.



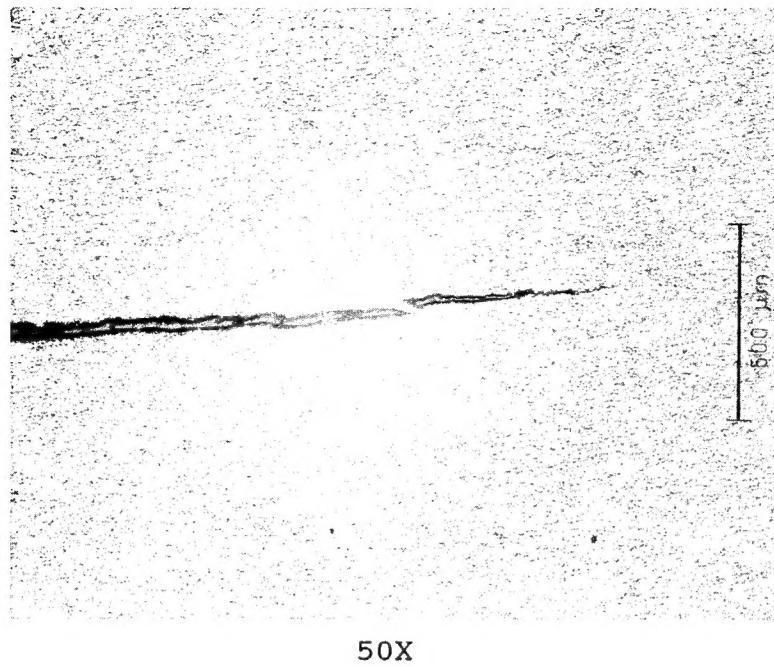
50X

Orientation to outer surface of liner



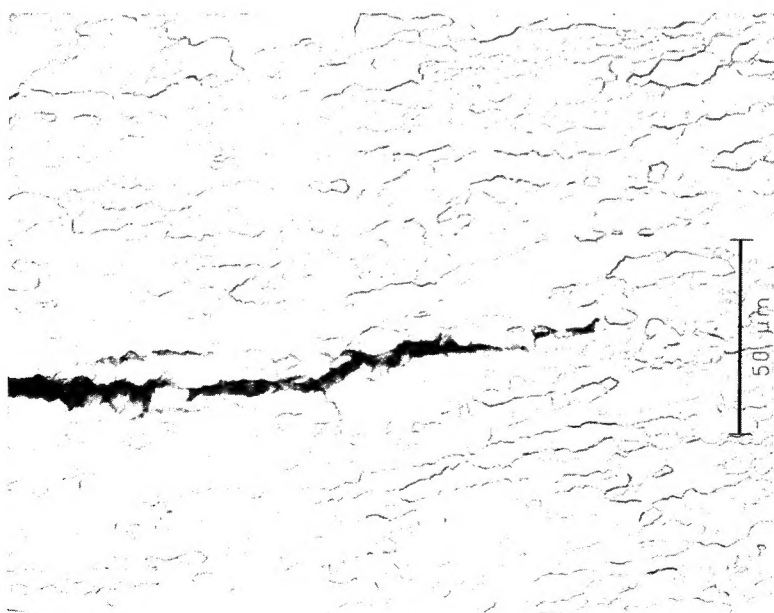
500X

Figure 43. Photomicrographs of crack in tungsten specimen W800-3 tested at 800°F.



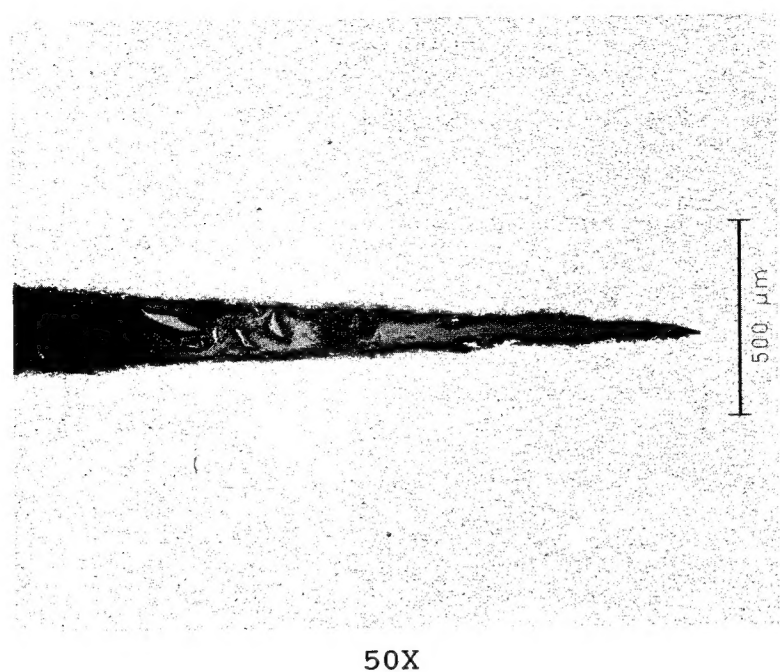
50X

Orientation to outer surface of liner



500X

Figure 44. Photomicrographs of crack in tungsten specimen W900-8 tested at 900°F.



Orientation to outer surface of liner

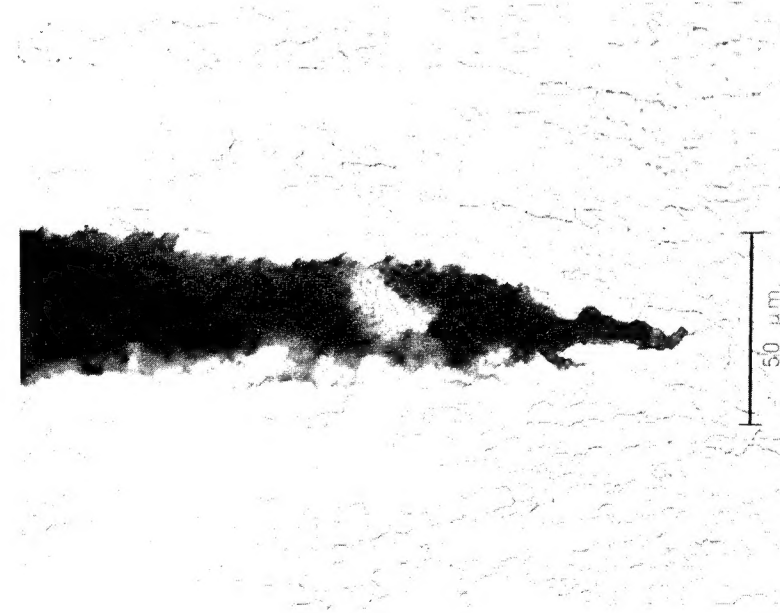


Figure 45. Photomicrographs of crack in tungsten specimen W1000-9 tested at 1000°F.

INITIAL DISTRIBUTION

Copies		Copies	Code
1	OCNR	1	0115
1	Code 225	1	60
		1	601
7	NAVSEA	1	602
1	SEA 03M	1	603
1	SEA 03M2	1	61
1	SEA 03P	1	61.1
1	SEA 03P1	1	612
1	SEA 03P2	1	613
1	SEA 03P41	1	614
1	SEA 99612	1	615
		1	615 (Franke)
		5	615 (Vassilaros)
5	DRPM	1	62
1	PMS 312	1	63
1	PMS 350	1	64
1	PMS 392	1	65
1	PMS 393	1	66
1	PMS 400	1	67
		1	68
2	DTIC	1	69
5	NSWC-Indian Head Division 10 Code 4140 (R. Garrett)		
5	NSWC, Dahlgren Division 5 Code R31 (H. Last)		